

REVIEW

Biological modification of mechanical properties of the sea surface microlayer, influencing waves, ripples, foam and air-sea fluxes

Ian R. Jenkinson^{*†}, Laurent Seuront[‡], Haibing Ding[§] and Florence Elias^{||,¶}

Gas exchange reduction (GER) at the air-sea interface is positively related to the concentration of organic matter (OM) in the top centimetre of the ocean, as well as to phytoplankton abundance and primary production. The mechanisms relating OM to GER remain unclear, but may involve mechanical (rheological) damping of turbulence in the water immediately below the surface microlayer, damping of ripples and blocking of molecular diffusion by layers of OM, as well as electrical effects. To help guide future research in GER, particularly of CO₂, we review published rheological properties of ocean water and cultures of phytoplankton and bacteria in both 3D and 2D deformation geometries, in water from both the surface layer and underlying water. Production of foam modulates air-sea exchange of many properties and substances, perhaps including climate-changing gases such as CO₂. We thus also review biological modulation of production and decay of whitecaps and other sea foam. In the ocean literature on biological production of OM, particularly that which associates with the sea surface, the terms “surfactant” and “surface-active” have been given a variety of meanings that are sometimes vague, and may confuse. We therefore propose a more restricted definition of these terms in line with usage in surface science and organic chemistry. Finally, possible changes in OM-modulated GER are presented in relation to predicted global environmental changes.

Keywords: Sea-surface microlayer; rheology; gas exchange reduction; phytoplankton; foam; organic matter

1. Introduction

For over a century, CO₂ levels in the atmosphere have been increasing at an accelerating rate. This increase is fuelled by anthropogenic CO₂ release, currently at over 9 billion tonnes annually (Le Quéré, 2015). As a greenhouse gas, CO₂ is leading to higher mean temperature on Earth (Friedlingstein et al., 2014) and in the world ocean, as well as increasing sea levels by thermal expansion and melting of ice caps (IPCC, 2014).

The Ocean absorbs about 25% of the anthropically produced excess CO₂ (Le Quéré et al., 2015). As a result, the

average surface ocean pH has decreased 0.1 units since the Industrial Revolution, i.e., a 30% increase in acidity (IPCC, 2014), and is predicted to fall another 0.3 to 0.4 units by 2100 if CO₂ emissions continue in a business-as-usual scenario (Orr et al., 2005).

In order to predict, manage and adapt to future changes in CO₂ dynamics, models of air-sea flux of CO₂ are being refined. This flux of CO₂ passes through the barrier of the sea surface microlayer (SML), here considered to be the top 50(±10) μm (Zhang et al., 1998). As the SML itself varies strongly in time and space in complex, non-linear ways, modelling the effects of the SML on CO₂ flux as a function of pertinent future scenarios is also important.

The importance of the SML in biologically modulating fluxes, particularly of CO₂, is increasingly appreciated, and has recently been reviewed by Wurl et al. (2016, 2017) and by Engel et al. (2017b). Therefore, the aim of this paper is to review known and suspected mechanical aspects of how biologically produced organic matter (OM) modulates air-sea fluxes of CO₂. We particularly address thalassorheological observations of biologically increased 3D viscosity and elasticity, 2D compression-dilation rheology, 2D shear rheology and foam dynamics.

* Institute of Oceanology Chinese Academy of Sciences, Qingdao, People's Republic, CN

† Agence de Conseil et de Recherche Océanographiques, La Roche Canillac, FR

‡ Centre National de la Recherche Scientifique, UMR 8187, Laboratoire d'Océanologie et de Géoscience, Wimereux, FR

§ Key Laboratory of Marine Chemistry Theory and Technology, Ministry of Education, Ocean University of China, Qingdao, People's Republic, CN

|| Laboratoire Matière et Systèmes Complexes (MSC) – Université Paris Diderot, CNRS UMR 7057, Paris, FR

¶ Sorbonne Universités, UPMC Université 6, UFR 925, Paris, FR

Corresponding author: Ian R. Jenkinson (ianjenkinson@qdio.ac.cn)

We review interactions among the biomodification of SML mechanical properties (2D and 3D rheology), waves, ripples, foam including whitecaps, and air-sea fluxes of gases and other materials and properties. After first clarifying the sometimes conflicting meanings of the key terms “surfactant” and “surface-active” (see **Table 1** for a glossary of other terms used in this review), we treat OM in the oceans, particularly in association with the SML. We follow with a section on the physics of the surface ocean, particular to the SML at the micrometre to nanometre scales, including mechanical (2D and 3D rheological) aspects. After relating bubbles and foam, including whitecaps, to OM and biological activity, we address poorly understood subjects, notably the effects of rough weather, and the problem of interactions among factors. To be forewarned is to be forearmed, so we look to the effects of future scenarios, treating warming, acidification, eutrophication, including harmful algal blooms and taxon change, and decreased deposition of black carbon, ending with general conclusions.

1.1. The meanings of “surfactant” and “surface active”

This section aims to clarify the meaning of “surfactant” as used in past literature on the ocean surface, and to help avoid misunderstandings in the context of future publications and research proposals in ocean science. The term “surfactant” has been used in the oceanographic literature with a variety of meanings that are sometimes vague. We suggest, as a more precise use of the terminology in future, that the noun “surfactant” and the adjective “surface-active” be restricted to the meanings used in chemistry. In chemical terminology, molecules of surfactant are amphiphilic. We suggest the definition, “A surfactant is a substance of which each molecule bears one or more functionally hydrophilic (polar) groups and one or more functionally hydrophobic (non-polar) groups. A further defining property of surfactants is that when they associate with a surface they reduce the surface tension, but other types of molecules can also have this effect.”

2. Organic matter (OM)

2.1. OM in the oceans

OM is frequently divided into particulate OM (POM) and dissolved OM (DOM), with a cut-off size at 0.45 μm (Nebbio and Piccolo, 2013). Sometimes, however, an intermediate class of colloidal OM (COM) is recognized, in which case DOM may be defined as passing through a 0.2- μm filter, while POM is classified as OM retained by a 0.8- μm filter (Alderkamp et al., 2007). The total amount of OM in the oceans is estimated at 662 Pg C (Hansell et al., 2009), or about 1.2 thousand billion tonnes of OM, but this represents only about 34 to 80 $\mu\text{mol kg}^{-1}$. A large proportion of this organic matter is polymeric, with complex molecules bearing lipid, amino-acid, carbohydrate and other functional groups (Van Vleet and Williams, 1983). In the ocean, DOM is partitioned into three relatively distinct pools: one refractory, with half-lives considered to be around 15,000 years; and one semi-labile (tens to hundreds of years), much of which remains in the surface mixed layers, particularly in the tropics, for several months or “a few

years”. The third pool consists of less than 1% of the total OM in the ocean, but it is very labile and so represents a large C flux (Hansell et al., 2009). We suggest that this fraction, generally close in space and time to areas of high productivity, is also the most rheologically active, both in the SML (Pogorzelski et al., 2005) and in the bulk phase (Jenkinson and Sun, 2010; Jenkinson et al., 2015).

2.2. OM and sea surface microlayer (SML) models

2.2.1. Oils calming troubled waters

Spreading oil on the sea surface to calm ripples has been recorded since ancient Roman times (Hühnerfuss, 2006). Franklin et al. (1774) described authenticated anecdotal reports, some written by Pliny the Elder, as well as Franklin’s own experiments on ponds, showing that small quantities of oil (sometimes olive oil) smooth ripples quickly and larger waves more slowly. In both the sea and in ponds small quantities of oil can smooth ripples quickly, but larger waves are damped more slowly (Alpers and Hühnerfuss, 1989).

2.2.2. The monolayer model

Some oils, including lipids and hydrocarbons, are buoyant, and all are hydrophobic. When hydrophobic liquids contact a water-gas interface, the water repels them; if their yield stress is lower than the external and internal stresses tending to deform them (i.e., they are functionally solid) and they are not confined laterally, they keep spreading on the plane of the water-gas interface until they form a monolayer. This spreading, however, can be reduced if the surface is already occupied by other molecules or if sufficiently strong stress, such as that due to wind, opposes it. Lucassen-Reynders and Reynders (1970) pointed out that monolayers reduce surface tension and may impart elasticity and viscosity to the surface film. As reviewed by Soloviev and Lukas (2014), the idea that a monolayer of OM molecules covers the sea-air interface influenced much research during the 1970s and 1980s, and was partly driven by problems of petroleum seeps and spills. The premise was that a molecular monolayer covers the sea surface with or without a thicker underlying layer of carbohydrate/protein or other types of OM. Many experiments were carried out and interpreted based on this monolayer assumption, and the mix of OM types in the SML were often liberally referred to as “surfactants”.

2.2.3. The gel layer model

Based on microscopical observations, the marine microbiologist and ecologist, John Sieburth (1983), hypothesized a surface layer of finite thickness and complex chemical and biological composition, in contrast to the molecular monolayer model. This gel-layer hypothesis has since been confirmed, both in slicks (Carlson, 1987) and in a more general context (Zhang et al., 1998; Cunliffe et al., 2013; Wurl et al., 2011, 2016, 2017).

2.3. OM in the SML and gas exchange reduction (GER)

2.3.1. Dissolved and colloidal OM (DOM and COM)

Part of the DOM in the ocean consists of exudates of various microalgae and macroalgae (Schilling and Zessner, 2011). Despite much progress in quantifying DOM

Table 1: A glossary of terms used in this review. DOI: <https://doi.org/10.1525/elementa.283.t1>

Acronym or symbol	Term	Units ^a	Remarks
– ^a	Gas film	–	Non-turbulent boundary layer on the gas side of a gas-liquid interface (Liss and Slater, 1974; Figure 1)
–	Gel	–	A substance that when subjected to a deformation stress $\tau < \tau_y$, where τ_y is the yield stress, deforms elastically. When the stress is removed, the material recovers its original shape. If a deformation stress $> \tau_y$ is applied, the material yields, and on removing the stress, the material's original shape is recovered only partly, if at all (Barnes et al., 1989).
–	Liquid film	–	Non-turbulent boundary layer on the liquid side of a gas-liquid interface (Liss and Slater, 1974; Figure 1)
–	Surfactant	–	As used by chemists and surface scientists for material consisting of amphiphilic molecules, i.e., molecules bearing both hydrophilic (polar) and hydrophobic (non-polar) terminations (Section 2)
–	“Surfactant” (in quotes)	–	Used here when citing authors who used the term “surfactant” in a variety of ways, generally as OM (whether surfactant or not) associated with the air-sea surface (Section 2)
CD	Compression-dilation of the sea surface film	–	This is also 2D strain
COM	Colloidal organic matter	–	Sometimes distinguished as intermediate between DOM and POM
DOM	Dissolved organic matter	–	Generally OM that passes through a 0.2- μm filter (Alderkamp et al., 2007)
EPS	Extracellular polymeric substances	–	
FD	Fluorescence depolarization	–	Technique used for measuring viscosity in seawater, including slicks (Sections 4.3.6, 4.5)
GER	Gas exchange reduction	%	–
MOA	Marine organic aggregate	–	–
OM	Organic matter	–	–
POM	Particulate organic matter	–	Generally OM that is retained by a 0.8- μm filter (Alderkamp et al., 2007)
SDR	Superhydrophobic drag reduction	–	In laminar flow of liquid, reduction of drag close to a hydrophobic sculptured wall (Section 4.3.2)
SML	Surface microlayer	–	Micrometre-scale vertical sampling of pH and other properties has shown a sharp gradient at a depth of $\sim 50 \mu\text{m}$ (Zhang et al., 1998, 2003b); conveniently, glass plate and Harvey stainless steel mesh samplers typically take a layer of thickness $\sim 50\text{--}80 \mu\text{m}$.

(contd.)

Acronym or symbol	Term	Units ^a	Remarks
TEP	Transparent exopolymeric substances	–	
TOC	Total organic carbon	mg m ⁻³	
TOM	Total organic matter	mg m ⁻³	As a rule of thumb TOM is often considered to be TOC × 2.
A	Area of a surface film constrained and controlled in a measuring apparatus	m ²	See definition for γ_{2D}
<i>a, b</i>	Parameters in Equation 3	–	Equation 3
<i>c</i>	The quantity <i>HC</i>	mole m ⁻³ (notionally)	Wanninkhof et al. (2009); Equation 1
C_{crest}	Forward speed of a breaking wave crest	m s ⁻¹	Section 5.4; Equation 8
<i>C</i>	Gas concentration	mol m ⁻³	Equation 1; Figures 1 and 2
C_a	<i>C</i> in air	mol m ⁻³	Wanninkhof et al. (2009); Figure 2
C_g	<i>C</i> in the bulk gas phase	mol m ⁻³	Figure 1
C_l	<i>C</i> in the bulk liquid phase	mol m ⁻³	Figure 1
C_{sg}	<i>C</i> at the gas side of a gas-liquid interface	mol m ⁻³	Figure 1
C_{sl}	<i>C</i> at the liquid side of a gas-liquid interface	mol m ⁻³	Figure 1
C_w	<i>C</i> in seawater	mol m ⁻³	Wanninkhof et al. (2009); Figure 2
<i>D</i>	Diffusion coefficient of a particular gas	m ² s ⁻¹	Equation 4
D_{air}	<i>D</i> of the gas in air	m ² s ⁻¹	After Equation 2
D_{water}	<i>D</i> of the gas dissolved in water	m ² s ⁻¹	After Equation 2
D_{eff}	The effective value of <i>D</i> compared with a calculated value	m ² s ⁻¹	Pogorzelski and Kogut (2001); Pogorzelski et al. (2005); Section 4.3.4
<i>G</i>	Modulus (i.e., stress) associated with straining in a 3D medium, used by rheologists for characterizing materials	Pa = N m ⁻²	<i>G'</i> , <i>G''</i> and <i>G*</i> are, respectively, the elastic (storage) modulus, viscous (loss) modulus and total modulus, such that $G^* = G' + iG''$, where <i>i</i> is the square root of -1 (Barnes et al., 1989; Ewoldt and McKinley, 2009); Sections 4.3.3, 4.3.4.
G_{2D}, G_{2D}^*	By analogy to <i>G</i> (above), modulus (stress) associated with dilation-compression in a 2D surface film	N m ⁻¹	As above, G_{2D} (or G_{2D}^*) may be decomposed into G'_{2D} and G''_{2D} ; Section 4.3.4; Equation 5.

(contd.)

Acronym or symbol	Term	Units ^a	Remarks
H	Henry coefficient of solubility of gas in a liquid	Dimensionless	Equation 1, Figure 2.
k	Diffusivity of gas	m s^{-1}	"Roughly proportional" to D (Liss and Slater, 1974); see Equation 2
k_a	Diffusivity on the air side such that $(k_c/\alpha) = 1/R_{air}$	m s^{-1}	Liss and Slater (1974), Wanninkhof et al. (2009); Equation 2
k_w	Diffusivity on the water side such that $(\epsilon k_w) = 1/R_{water}$	m s^{-1}	Liss and Slater (1974), Wanninkhof et al. (2009); Equation 2
M_w	Molecular mass	$\text{Da} = \text{g mol}^{-1}$	–
n	Power-law dependence of k on U_{10}	Dimensionless	Equation 3
N	Avogadro's number	6.02×10^{23} molecules mol^{-1}	Equation 4
P	Radius of a molecule	nm	$\sim 0.3 \text{ nm}$ for hydrated solute molecules of CO_2 or O_2 ; Equation 4; Section 3.3.2
R	SML resistance to vertical gas flux	s m^{-1}	Liss and Slater (1974); text after Equation 2
R_{air}	"Air-side" resistance	s m^{-1}	Liss and Slater (1974); text after Equation 2
R_{water}	"Water-side" resistance	s m^{-1}	Liss and Slater (1974); text after Equation 2
RR	Universal gas constant	$8.31 \text{ J mol}^{-1}\text{K}^{-1}$	Equation 4
T	Temperature,	$^{\circ}\text{C}$, except where	Equation 4
T_s	Seawater temperature	otherwise stated	
t_{bub}	Persistence time of a bubble in a whitecap	s	Section 5.2
U_{10}	Wind speed at a notional height of 10 m above water level	m s^{-1}	Section 3.3.1. et seq.
W, W_A, W_B	Coverage fraction by total whitecaps, type A whitecaps and type B whitecaps, respectively	%	Section 5.4; Equations 5, 6, 7 and 8
α	Ostwald solubility coefficient of a gas in a liquid	Dimensionless	Wanninkhof et al. (2009); Equation 2
$\Delta\tau_{2D}$	Change in stress in the surface film associated with changes in dilation-compression	N m^{-1}	Section 4.3.4 et seq.
ϵ	A chemical "enhancement factor", also referred to as "gas reactivity"	Dimensionless	Wanninkhof et al. (2009); Equation 2

(contd.)

Acronym or symbol	Term	Units ^a	Remarks
γ	Shear in a 3D material. (Shear is a particular geometry of strain)	$m\ m^{-1}$, i.e., dimensionless	Simple shear (Barnes et al., 1989)
$\dot{\gamma}$	Strain rate, including shear rate	$m\ m^{-1}\ s^{-1} = s^{-1}$	
γ_{2D}	Dilation-compression strain in a 2D film, equal to dA/A	$m\ m^{-1}$, i.e., dimensionless	The use of the "2D" notation avoids the need to define the thickness of a film, such as the SML; Section 4.3.4 et seq.
γ_{2D}^{shear}	Shear in a 2D film	$m\ m^{-1}$, i.e., dimensionless	Section 4.3.5
γ_{2D}^{shear}	Shear in a 2D film	$m\ m^{-1}$, i.e., dimensionless	Section 4.3.5
$\dot{\gamma}_{2D}$	Dilation-compression strain rate in a 2D film area	$m^2\ m^{-2}\ s^{-1} = s^{-1}$	$=d\gamma_{2D}/dt$; Section 4.3.4 et seq.
η	Viscosity of a 3D medium	$Pa\ s = N\ s\ m^{-2}$	Equation 4, Section 3.3.2 et seq.
$\eta_{2D,shear}$	2D viscosity associated with shearing in the surface film	$N\ s\ m^{-1}$	Section 4.3.5 et seq.
$\lambda(c_{crest})d c_{crest}$	Length of breaking wave crests per area of ocean surface	$m\ m^{-2} = m^{-1}$	Equation 8
τ	Shear stress due to shearing in a 3D medium	$N\ m^{-2}$	Section 4.3.1 et seq.
τ_{surf}	Surface tension	$N\ m^{-1}$	Section 4.3.1 et seq.
τ_{2D}	Stress associated with dilation-compression of the surface film	$N\ m^{-1}$	Section 4.3.1 et seq.
$\tau_{2D,shear}$	Stress associated with shearing of the surface film	$N\ m^{-1}$	Section 4.3.4
			Section 4.3.5

^a A dash (-) in the "Units" column denotes "dimensionless".

and POM and its constituents in the last three decades (Nebbioso and Piccolo, 2013), the proportions of their components including carbohydrates, lipids and proteins are still uncertain. It is clear, however, that many are surfactants *sensu stricto*, as defined in **Section 1.1**. Carbohydrates are dominant in terms of mass, followed by proteins and thirdly by a lipid class comprised of free fatty acids, free fatty alcohols and triglycerides. However, lipids affect the surface electric potential and film pressure of multicomponent films much more strongly than carbohydrates or proteins in relation to their relatively low abundance (Van Vleet and Williams, 1983).

The surface of water or saltwater at an interface with OM-free air possesses surface tension. This tension, by allowing the surface to compress and dilate almost without the dissipation of viscous energy, supports the propagation of surface ripples, which compress and dilate the interface. Adding surfactants to seawater-air interfaces reduces surface tension without eliminating it: ripples can still propagate. However, many surfactants form aggregates or films that have been shown to increase the 2D dilational viscosity of the surface (Jarvis et al., 1967) and to damp capillary waves (Deacon, 1979), presumably by viscous energy dissipation to heat. Goldman et al. (1988) added real surfactants to seawater collected from the NW Atlantic, and showed that they reduced O_2 exchange (O_2 GER) in laboratory measurements. These authors also found that natural OM (which they also called “surfactants”) in the SML of these waters was positively related to GER. Frew et al. (1990) used identical methods to measure O_2 GER in filtered and unfiltered cultures of seven marine algal species diluted with either distilled water or natural seawater. Finite O_2 GER always occurred relative to culture-medium controls, with values of $(1/GER) = (O_2 \text{ flux in experimental material}) / (O_2 \text{ flux in control})$ ranging from 58% to 100% (their **Figure 3**). The term $(1/GER)$ showed a non-linear negative relationship with total organic carbon concentration [TOC], but also showed a high-scatter intercept around 74%, suggesting that both [TOC] and unknown factor(s) played comparably important roles in reducing O_2 exchange. The authors also measured 3D shear viscosity at a high shear rate of 73.4 s^{-1} (Brookfield LVTD viscometer) at 20°C . Relative to culture-medium controls, algal treatments increased viscosity from ~ 0 to $\sim 400\%$, the highest being for *Porphyridium* culture (their Tables 2 and 4), but viscosity showed no clear relationship with GER.

Calleja et al. (2009) used an *in-situ* floating device to measure air-sea CO_2 exchange in the NE Tropical Atlantic and off the Antarctic Peninsula at 10-m altitude wind speeds (U_{10}) of $1\text{--}12 \text{ m s}^{-1}$. They compared measured to modelled values of gas exchange rate (i.e., gas exchange speed $|k|$) and thereby effectively derived GER. Their findings show that [TOC] was positively related to GER at U_{10} values of $1\text{--}5 \text{ m s}^{-1}$, and that GER values also co-varied seasonally and geographically with marine productivity. The authors found [TOC] at 5 m depth to range from 40 to $125 \mu\text{mol C L}^{-1}$, with corresponding [TOC] in the top 2 cm ranging from 8% lower to 73% higher. CO_2 residual flux over a range of [TOC] from 60 to $120 \mu\text{mol C L}^{-1}$ showed

a strong negative relationship with [TOC] in the top 1 cm (Calleja et al., 2009; their **Figure 4**). The authors concluded that the total organic carbon concentration [TOC] at the water surface suppresses air-sea CO_2 gas fluxes at wind speeds at least up to 5 m s^{-1} . [TOC] was found to be associated with reduced fluxes of other gases rather similarly, and they suggested that this may apply not only in the areas they studied but over the world ocean. In this respect, Sabbaghzadeh et al. (2017), in two transects in the Atlantic from 50°N to 50°S , found little or no relationship between U_{10} and the enrichment factor of “surfactant” concentration in the SML relative to that in 7-m deep subsurface water. Measurements were made at U_{10} values ranging from 0.5 to 13 m s^{-1} , and this implies that such wind speeds cause little or no “mixing down” of the surface-associated OM.

Liss and Slater (1974) proposed a simplified equilibrium model of air-sea gas exchange in which gas transfers through two non-turbulent boundary layers in series, one on the gas-side of the gas-liquid interface, and the other on the liquid-side (**Figure 1**). The gas concentrations on the gas-side (C_g) and on the liquid-side (C_l) of the gas-liquid interface are different in proportion to the solubility of the gas in the liquid (Henry’s Law). A quantity c may be calculated such that:

$$c = H C \quad (1)$$

where H (the Henry’s law coefficient) = [equilibrium concentration in the gas phase (g cm^{-3} of air)]/[equilibrium concentration of un-ionized dissolved gas in the liquid phase (g cm^{-3} of water)] for the particular gas, which is closely related to $1/\alpha$, where α is solubility in the liquid, and C is the gas concentration (**Figure 2**). Values of α in seawater are given for several gases by Wanninkhof et al. (2009).

Wanninkhof et al. (2009) modified Liss and Slater’s model by plotting c rather than C across the SML (**Figure 2**). In this model, as long as the interface itself provides no resistance to diffusion (e.g., by OM) then c is the same at the air side and the liquid side of the interface. The total resistance to transfer is therefore the sum of the respective resistances in the air and water diffusive sublayer (boundary layer); k^{-1} is proportional to the total resistance:

$$k^{-1} = (k_a / \alpha)^{-1} + (\varepsilon k_w)^{-1}, \quad (2)$$

where $k_a / \alpha = 1/R_{air}$, where R_{air} is the air-side resistance, and $\varepsilon k_w = 1/R_{water}$, where R_{water} is the water-side resistance. The terms k_a and k_w have the units of velocity (Liss and Slater, 1974) (because they represent transfer across a large 2D surface rather than in 3D), and they are roughly proportional to D_{air} and D_{water} , the respective diffusion coefficients ($\text{m}^2 \text{ s}^{-1}$) of gas in air and of dissolved gas in water. In both the Liss-Slater and Wanninkhof models the interface is implicitly of zero thickness. In reality in the gas film and the liquid film are unlikely to be as well defined as in these two models or to show in general linear gradients of concentration as depicted in **Figures 1** and **2**. While the

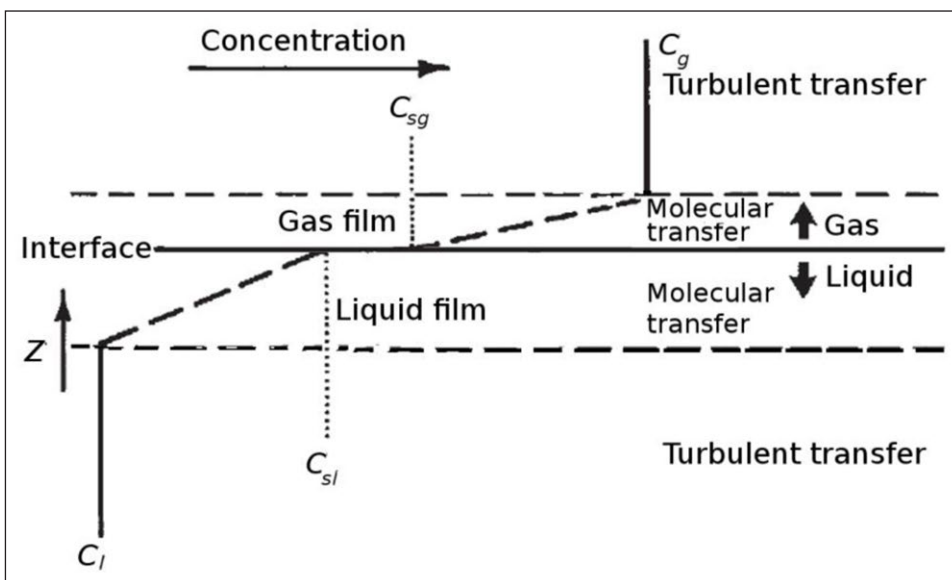


Figure 1: Simplified conceptual two-layer equilibrium model of air-sea gas exchange. In this sketch, net transfer from air to sea is assumed. C_l and C_g are gas concentrations in the bulk phase of the liquid and gas phases, respectively. C_{sl} and C_{sg} are the concentrations, respectively, at the liquid-side and the gas-side of the gas-liquid interface. Note that $C_{sl} < C_{sg}$ because solubility of the gas in the seawater phase is $< 100\%$. (Inspired and somewhat reconceptualised from Liss and Slater, 1974). DOI: <https://doi.org/10.1525/elementa.283.f1>

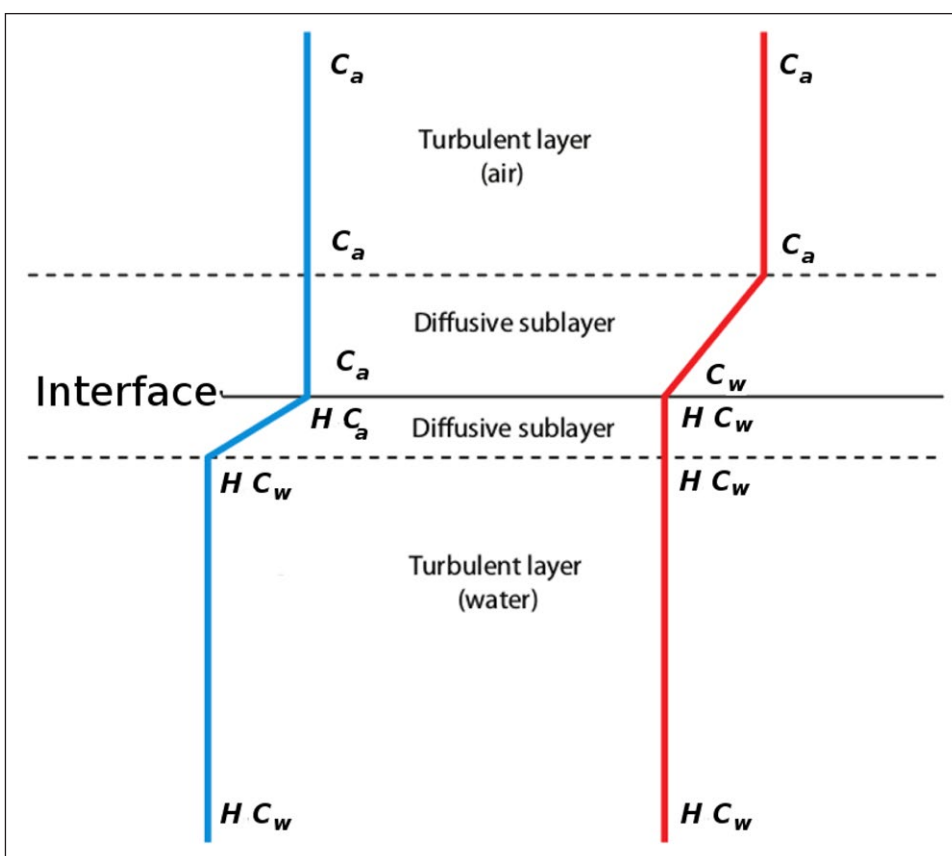


Figure 2: Conceptual view of boundary layer concentration profiles. Resistance to gas transfer is concentrated in the diffusive sublayers. On the left (blue line) is the activity profile for an insoluble gas with the resistance in the aqueous-side diffusive sublayer. On the right (red line) is the profile for a soluble gas with resistance in the air-side diffusive sublayer. Soluble gases have an Ostwald solubility > 100 . The figure assumes no resistance to diffusion (e.g., by OM) at the interface. C indicates gas concentration; H , Henry coefficient of solubility; subscript a , in air; and subscript w , in seawater. (Redrawn and reconceptualised from Wanninkhof et al., 2009). DOI: <https://doi.org/10.1525/elementa.283.f2>

diffusive sublayers (**Figure 2**) need further modeling and *in situ* investigation, the key determinants of gas transfer speed k are likely to be the concentration gradients on both the water- and air-sides where they intercept with the interface.

As Liss and Slater (1974) suggested, any contaminants would contribute to the resistance of the phase in which they occur. The work of Goldman et al. (1988) and of Calleja et al. (2009), both discussed above, has empirically strongly supported Liss and Slater's earlier conjecture.

The transfer velocity k of gases with $\alpha > \sim 100$, for gases that react rapidly in water, is controlled by processes on the airside of the interface, and not on the waterside (Liss and Slater, 1974; Wanninkhof et al., 2009; **Figure 1**). For gases with values of $\alpha < \sim 1$, as well as those with high reactivity ε , however, k is limited by processes on the waterside. For CO_2 , which has a low to intermediate value of α (0.727) at 20°C and 35 psu (Wanninkhof et al., 2009) and a high value of ε , k may thus be controlled by processes on both sides of the interface.

While consideration of GER in this section has, for simplicity, mainly assumed a stagnant-water model, gas flux and GER in the real ocean take place under a wide range of meteorological, hydrological and biological conditions. Wanninkhof et al. (2009) have reviewed much work on determining k for CO_2 and other gases under calm and moderate wind speed conditions (U_{10}) *in situ* and in the laboratory (considering calm conditions as 0–3.6 m s⁻¹, moderate as 3.6–13 m s⁻¹, and rough as >13 m s⁻¹). Under moderate conditions, work at sea becomes more difficult, and laboratory simulations perhaps less realistic. Determination of k in calm and moderate conditions generally gives a power law relationship:

$$k = b + a U_{10}^n, \quad (3)$$

where b represents k under stagnant conditions, and n lies between 2 and 3, with an empirically determined coefficient a . Measured values, however, give considerable scatter, and an unknown fraction of this scatter may be due to GER produced by biopolymers (Calleja et al., 2009). Under calm and moderate winds, understanding of air-sea exchange of gases, heat, humidity, momentum as well as wave propagation and foam formation will be improved in future by more sophisticated, high-speed, high-resolution 3D filming of surface processes, and may improve phenomenological understanding of CO_2 k .

Polymer molecules tend to be rheologically active. In 3D, particulate, colloidal and dissolved polymers in ocean water, including transparent exopolymeric particles (TEP) and organic aggregates (OAs), produce elasticity and increase viscosity in the bulk phase of both underlying water and in water sampled from the SML. In 2D, by binding electrically to or otherwise associating with the surface film, they produce viscosity in it (Van Vleet and Williams, 1983) and change its elasticity both in the SML and on the surfaces of bubbles and droplets.

As much DOM and TEP and many OAs are sticky or surface-active, and in some cases buoyant (Riebesell, 1992;

Mari, 2008), a fraction of this material accumulates at the surface. The hydrophobic (non-polar) fraction largely becomes electrically bound to the surface (Žutić et al., 1981; Čosović et al., 2005), while the hydrophilic (polar) fraction will be electrically repelled by it (van Oss et al., 2005), but may float by buoyancy just below it. Surfactant *sensu stricto* molecules will tend to become incorporated into the film just below the hydrophobic fraction. This organic surface “film” material is visible in calm weather when it forms slicks, which have marked surface rigidity, causing structure in the water surface at scales that can exceed 100 m and 100 min when the sea is calm (Peltzer et al., 1992; **Figure 5**).

In surface samples taken from the NW Atlantic, from coastal waters of the USA to a point about 1000 km offshore near Bermuda, as well as in some from the Caribbean, Goldman et al. (1988) measured O_2 GER under turbulent conditions in the laboratory. They found that O_2 GER values related to surface OM, which they called “surfactant”, and they were much higher for inshore samples (~50%) than for offshore samples (~10%). Calleja et al. (2009) compared GER (CO_2) in spring, summer and autumn in the North Atlantic and the Southern oceans, at wind speeds up to 5 m s⁻¹, and found GER positively related to total organic matter (TOM) in the top cm or so, covarying also with marine productivity. Precise measurement of gas exchange at higher wind speeds is crucial but remains difficult.

Assuming that the covariation between OM concentration and GER across the SML is because the OM actually causes GER, then what is the mechanism? Two classes of mechanism appear the most plausible: 1) reduction in vertical movement of water containing the dissolved gas by partial gelling (increased elasticity) in and/or near the SML (Jenkinson, 1993b; Jenkinson and Biddanda, 1995); and 2) reduction of molecular diffusion of the gas due to obstruction by molecules or larger structures of OM. Two further mechanisms might also be possible: 3) adsorption of the gas onto OM molecules; and 4) electrical effects close below and/or close above the air-sea surface. We next consider these four possible mechanisms.

Concerning the boundary between the turbulent layer and the diffusive sublayer on both sides (water and air) of the air-sea interface (**Figure 2**), such boundaries still remain complex and difficult to model (Adrian, 2010; Marusic et al., 2010). The presence of biopolymers of various rheological and surface properties complicates the situation even further. We suggest that there is a long way to go before models incorporating the diffusive and turbulent fluxes, particularly on the water side of the air-sea interface, can be adequately conceived and tested. The “economical” approach – assuming OM does not affect fluxes – has now been shown false. Therefore, while the difficult phenomenological models of turbulence and rheology are catching up, the best way forward may be empirical laboratory and field measurements of fluxes within the ambient envelope of physical and biological sea-surface conditions over a wide range of scales.

2.3.2. Gel and non-living POM

The Einstein relation states that the diffusion coefficient:

$$D = RR T / (6 \pi \eta N P), \quad (4)$$

where RR is the universal gas constant ($8.31 \text{ J mol}^{-1} \text{ K}^{-1}$), T is temperature (Kelvin units), η is the viscosity (Pa s), N is Avogadro's number (6.02×10^{23}), and P is the hydrated radius of the solute molecules ($\sim 0.3 \text{ nm}$ for CO_2 and O_2) (Conlisk, 2013). This relationship is very well known, but it was derived for systems with only small, roughly spherical molecules. For polymeric systems, applying this relationship is generally inappropriate. Where the polymers form a gel-type network of fibrils, molecules smaller than the mesh size between the fibres will diffuse more or less unhindered (Sonnenburg et al., 1990), while the gel network adds elasticity to the material at length scale larger than mesh length scale. The dependence of D on η in polymer solutions and gels thus becomes a function of length scale and geometry. In such cases neither viscosity nor diffusion coefficient can be predicted from **Equation 4**, and measurements need to be conducted case by case at the scale(s) and geometry(ies) appropriate to the problem in hand. However, extending the approach of Calleja et al (2009) might be more pragmatic.

2.3.3. Living POM

Anthropically driven eutrophication and climate change are leading to increasing biomass of phytoplankton in coastal waters (Glibert et al., 2005), in particular the occurrence of taxa such as *Karenia mikimotoi*, *Phaeocystis* spp. and *Ostreopsis ovata* (Lassus et al., 2016), which markedly increase seawater viscosity, while *Phaeocystis* also produces large quantities of foam (Seuront et al., 2006; Jenkinson et al., 2015; Giussani et al., 2015). Engel et al. (2017a) found that blooming of *Phaeocystis pouchetii* in Arctic waters east of Greenland are also strongly associated with massive production of TEP (up to several hundreds of $\mu\text{g Xeq L}^{-1}$). *Phaeocystis antarctica* also blooms over huge swathes of the Southern Ocean (Smith et al., 2003; Seuront et al., 2010), and floating macroalgae, including *Enteromorpha prolifera* (Zhou et al., 2015) and *Sargassum* spp. (Smetacek and Zingone, 2013) are increasing around the world. These algae may be modifying surface properties, gas exchange and wave propagation not only by OM secretion but also directly by the mechanical properties of their filaments and thalli which may hinder diffusion. Filamentous cyanobacteria such as *Trichodesmium* spp. float on the surface of many oceans (Capone et al., 1997), as do *Aphanizomenon* spp. and *Nodularia spumigena* in the Baltic (Ploug, 2008) and some Phycoma stages of species of the prasinophyte *Halosphaera* (Jenkinson, 1986b; Thronsen, 1996) in the North Atlantic.

2.4. Conclusions concerning OM

The huge pool of OM in the oceans, over 1×10^{12} tonnes, represents only a mean concentration of $\sim 40 \mu\text{mol C kg}^{-1}$ in the water. It consists predominantly of DOM. For thousands of years, the effect of adding oil to ocean and lake water has been observed to calm the surface,

predominantly ripples. As addition of oil was observed to spread rapidly on the surface to form what could be calculated as a molecular monolayer, early models of ripple and wave damping, as well as gas exchange by oils, solvents and natural OM were based on the concept of a monolayer of OM at the surface. For natural OM, such a monolayer was generally assumed to be dominated by lipid. Later, biologists contributed observations of the SML, showing that it consists of a characteristic ecosystem, is composed of an OM layer more like a gel, and is thicker than previously thought. This gel-type material consists principally of carbohydrates and proteins as well as lipids. Many of these components are present as terminations on the same polymeric molecules. Most ocean DOM is refractory, having a half-life estimated at thousands of years, but a small part (<1%) is labile (hours to days), and thus represents a proportionately large C flux.

Much work on the 2D dilation-compression rheology (dynamic surface tension studies) of the SML, carried out in the 1980s and 90s (and reviewed here), was also accompanied by some work on SML rheology combined with work on GER. Most of this work addressed O_2 , but the findings also seem relevant to CO_2 GER. This work and later, more extensive, work has found GER to co-vary with OM in the SML, as well as with primary production.

Study of the physical structure of the SML in relation to gas diffusion and solubility dynamics has been dominated by models, with experimental verification notably by Liss and Slater (1974), and later by Wanninkhof and co-workers (Wanninkhof et al., 2009, and citations therein). Such work needs to continue, combined with that on the effects of OM on GER.

Considering living POM, the little work on the effects of different phytoplankton species on both 3D and 2D thalassorheology, as well as on gas exchange, has shown huge differences among species. This work is particularly important as it suggests that switches in species dominance could have large effects on gas diffusion and aerosol production, especially as the climate changes.

Finally, lipids affect the surface electric potential of the surface proportionately more than other OM components in relation to their abundance. This electrical potential effect due to lipids and other OM is not included in detail in the present review, but may be very important in determining surface film dynamics, and thus GER. Earlier electrochemical studies have not been followed up; this field may require greater diligence, particularly in relation to GER, aerosols and climate change.

3. SML physics

3.1. Some mechanisms for reduction of vertical water movement in and near the SML

Close to the air-sea surface, vertical movement of water is produced by both cooling and evaporation at the surface, two often negatively correlated processes, as well as any turbulence forced from the water below or from the air above. Defined relative to the surface, and neglecting rain and evaporation, upward and downward movement of water has to be equal, and must involve lateral water

movement as well, necessarily forming circulation cells and patterns, potentially detectable at the surface. Vertical water movement is resisted by the two main stratifying mechanisms, input of heat (solar radiation or warm air) or freshwater (rain, snow, runoff from land, melting ice, condensation of water vapour) to the surface. Quantification of these processes, to be most useful, must be made at the scales involved in them. Some types of OM, notably those forming networks of polymer fibrils or even larger structures such as thalli of floating macroalgae, are likely to increase viscoelasticity and hence resist water movement thus damping turbulence (Jenkinson, 1986a, 1993a, 1993b). Similarly, the scales of these structures and of any resistance they make to water movement must be correctly identified and used in measurements and modelling. Anisotropic horizontal layering of structures is likely to be the most effective geometry in resisting vertical water movement. Conversely, output of heat (outward radiation, cold air) or loss of water (evaporation) from the surface to the air increases density and reduces or even destroys stability.

3.2. Micrometre- and nanometre-scale physics

The air side of water-air interface may be considered as the most hydrophobic, non-polar surface known (van Oss et al., 2005). When surfactant molecules get sufficiently close to a water-gas surface or a water-oil surface, they orientate with the hydrophobic heads projecting into the hydrophobic phase and the hydrophilic tails into the water phase. This molecular-scale attraction to the surface pushes them to spread out on the surface to form a monolayer unless opposed by other sufficiently strong forces, such as wind drag. By comparison, when hydrophobic molecules get sufficiently close, a few nanometres (van Oss et al., 2005), to a water-gas or a water-oil surface, molecular-scale forces attract them into the oil or gas phase. Correspondingly, on the water side of such an interface, polar molecules, such as sugars and neutral salts are then sterically excluded from the surface, leaving a layer of essentially pure water a few nanometres thick. Any surfactant macromolecules larger than a few nanometres, however, would span the otherwise pure layer. If the water-gas surface is the SML of a calm sea, gravity will oppose this repulsion so that the oil or lipid (if pure) would sit suspended slightly (a few nanometres) above the surface without binding to it. This hydrophobic repulsion may allow drag reduction to occur between the hydrophobic surface layer and the underlying water and dissolved, colloidal or particulate polar material. If hydrophobic material but no surfactant is present at the interface, then a slip layer of functionally reduced viscosity between the water and hydrophilic matter on the one hand and the overlying hydrophobic matter on the other could result, as proposed by Jenkinson and Sun (2014) to explain laminar drag reduction found in cultures of bacteria and marine microalgae. The thickness of this slip layer would depend on the degree of hydrophobicity and on the details of roughness of the hydrophobic surface (Rothstein, 2010).

3.3. *Thalassorheology of ocean water in the top 100 m and the top 1 mm*

3.3.1. General considerations

In 3D geometries, the rheological (“thickening”) effects of OM in the SML, and in the metre or so below it, have been assessed by both viscometry and rheometry measurements and reported as increases in seawater viscosity η , as stress τ vs. shear γ , and/or as τ vs. shear rate $\dot{\gamma}$, and in capillary-tube-flow. In 2D geometries, dilational rheometry (also known as dynamic surface tension measurement) measures and reports changes in surface tension τ_{surf} vs. surface dilation-compression strain γ_{2D} and/or as τ_{surf} vs. surface dilation-compression strain rate $\dot{\gamma}_{2D}$.

3.3.2. Organic matter and the mechanical (rheological) properties of the SML

The most labile pool of DOM in the oceans consists of less than 1% of the total DOM, but its very lability represents a large C flux. This labile DOC pool is variable in molecular composition, from one location to another, but the major part of it originates from secretions and cell breakdown in the primary-production-driven food web. It consists of acid and neutral carbohydrates, lipids, proteins, nucleic acids and other organic molecules, but the exact proportions of its components are still poorly known due to difficulties in marine OM analyses, despite major recent advances. Much of the labile pool of DOM is known to be in rapid exchange with TEP, active at surfaces and, like TEP, generally sticky (Mari et al., 2016). The labile pool is believed to be the part of DOM mainly responsible for both elasticity and for the non-Newtonian “excess” viscosity, not due to water and salts alone, in the seawater bulk phase (Jenkinson, 1993b; Jenkinson and Sun, 2010; Jenkinson et al., 2015). For instance, Jenkinson and Biddanda (1995) found that elasticity and excess viscosity were positively related to chlorophyll concentration at scales of metres to thousands of kilometres.

Surface effects on the cellular surfaces of plankton, including possible superhydrophobic drag reduction (SDR), have been addressed by Jenkinson (2014). The sea surface, too, is hyperhydrophobic (van Oss et al., 2005), and the implications of this characteristic are considered in **Section 4.3.4**.

3.3.3. Differing effects of taxa, physiological state and life stage

Some marine (Jenkinson, 1986a, 1993a) and freshwater (Petkov and Bratkova, 1996) phytoplankton species in culture have been found to contribute strongly to 3D elasticity and excess 3D viscosity, but others had less or no measurable effect, suggesting that differences between species, and perhaps physiological state, may add variance to the above-mentioned relationship between viscoelasticity and chlorophyll concentration. Jenkinson and Sun (2010) have summarized these measurements.

Portela et al. (2013) and Patricio et al. (2015) made rheological measurements on cultures of the bacterium *Staphylococcus aureus*. As in *Phaeocystis* (Seuront et al., 2007), these bacterial cultures showed viscosity that

changed markedly with growth phase, and not simply with cell density or time. The viscous modulus G'' and the elastic modulus G' showed different power-law relationships with shear rate, as in the different planktonic algae measured by Jenkinson (1986a). In bacterial cultures, the power law exponents also changed as a function of growth phase. These observations suggest a promising area of research, as similar work following life cycle stages in cultures of phytoplankton would be easy to implement.

3.3.4. 2D dilational rheological properties of the surface film

The accumulation of buoyant, hydrophobic or amphiphilic material at the surface of water lowers the apparent surface tension of water. Compared to the air interface of most other liquids, that of pure water shows an exceptionally high surface tension, $-\tau_{surf} = 72.8 \text{ mN m}^{-1}$ at 20°C (van Oss et al., 2005). A drop of floating hydrophobic material deposited on water reduces $|\tau_{surf}|$ locally. The local gradient of surface tension generates a net force that tends to spread the drop from the low surface tension region towards the high surface tension region. This tendency explains why, when a drop of low-viscosity oil or soap solution is spread on a calm pond, the surface rapidly withdraws from the position of the drop. If the oil or soap has high viscosity, however, the withdrawal will be slower.

Using an apparatus similar to those in **Figures 3** and **4**, a range of workers (e.g., Dragčević et al., 1979; Dragčević

and Pravdić, 1980, 1981; Williams et al., 1980, 1986; Van Vleet and Williams, 1983; Goldman et al., 1988; Frew and Nelson, 1992a, b; Frew et al., 2006) have compared the 2D rheological properties of both surface “film” samples taken with a stainless steel mesh sampler with samples taken by bottle from depths of 0.5 m and 5m. Oscillation of the wiper (slider) in the apparatus gave Lissajous plots (Ewoldt and McKinley, 2009) of τ_{2D} vs. γ_{2D} (not shown), where the strain $\gamma_{2D} = dA/A$ is the relative variation of the total area in the experiment. As the wipers compressed the surface-film material, the apparent surface tension τ_{2D} measured by the Wilhelmy plate decreased by an amount $\Delta\tau_{2D}$ up to 6.6 mN m^{-1} for the surface “film” of water itself sampled from the surface “film” *in situ*, but only 0.06 mN m^{-1} for water from 5m depth (**Figure 6**). $\Delta\tau_{2D}$ represents the total resistance by the surface layer to compression. It increases during compression, pushing back against this compression. By analogy with the pressure of a 3D gas (but with a change in dimensions from $\text{Pa} = \text{N m}^{-2}$ to N m^{-1}), the difference $\Delta\tau_{2D} = \tau_0 - \tau_{2D}$ is called the surface pressure of the microlayer. The compressive motion of the wiper was stated by the authors to be sinusoidal. The peak in compression rate $dy_{2D}/dt = \dot{\gamma}_{2D}$ therefore occurs at mid-trajectory, $\gamma_{2D} = 1.25$. Such behaviour is typical of a visco-elastic material described by a surface viscoelastic modulus G_{2D}^* , such that $\Delta\tau_{2D} = G_{2D}^* \gamma_{2D}$. G_{2D}^* is a complex quantity, $G_{2D}^* = G'_{2D} + iG''_{2D}$, the real part G'_{2D}

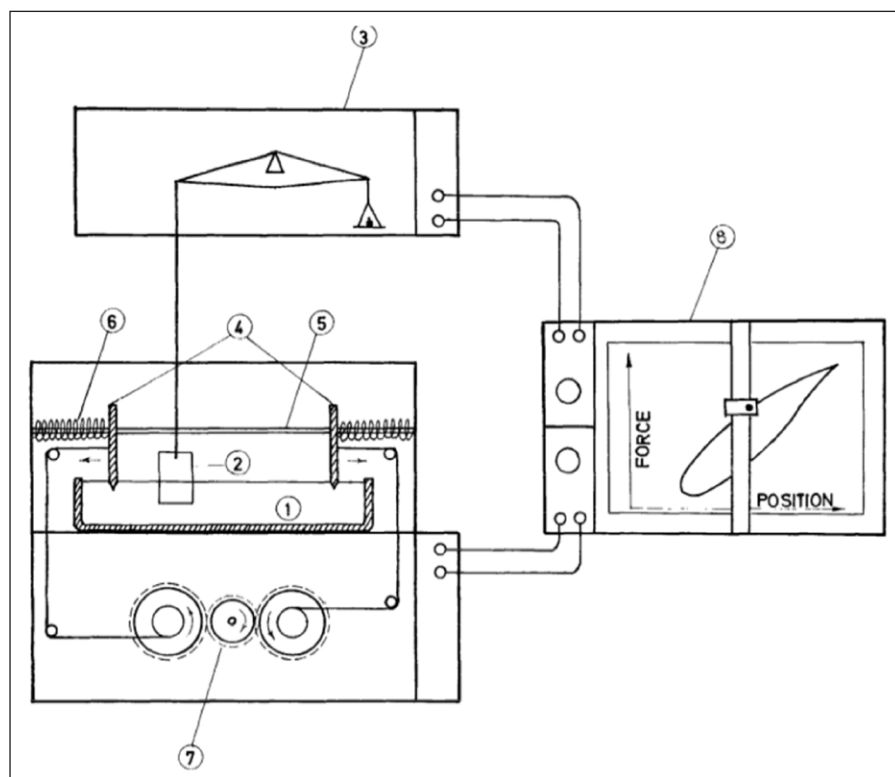


Figure 3: Apparatus for measuring dilation rheology of the surface film. The depicted setup is to measure water-air dynamic surface tension (allowing surface visco-elasticity to be determined) with a Langmuir trough (aluminium lined with polytetrafluoroethylene [PTFE; i.e., Teflon]): 1 – rectangular sample trough; 2 – platinum-foil Wilhelmy plate; 3 – microbalance; 4 – twin oscillating PTFE blades; 5 – guide for blade travel; 6 – springs forcing blades towards centre of trough; 7 – motor-operated pulley opposing force exerted by the springs; 8 – chart recorder. For further details see Dragčević et al. (1979). DOI: <https://doi.org/10.1525/elementa.283.f3>

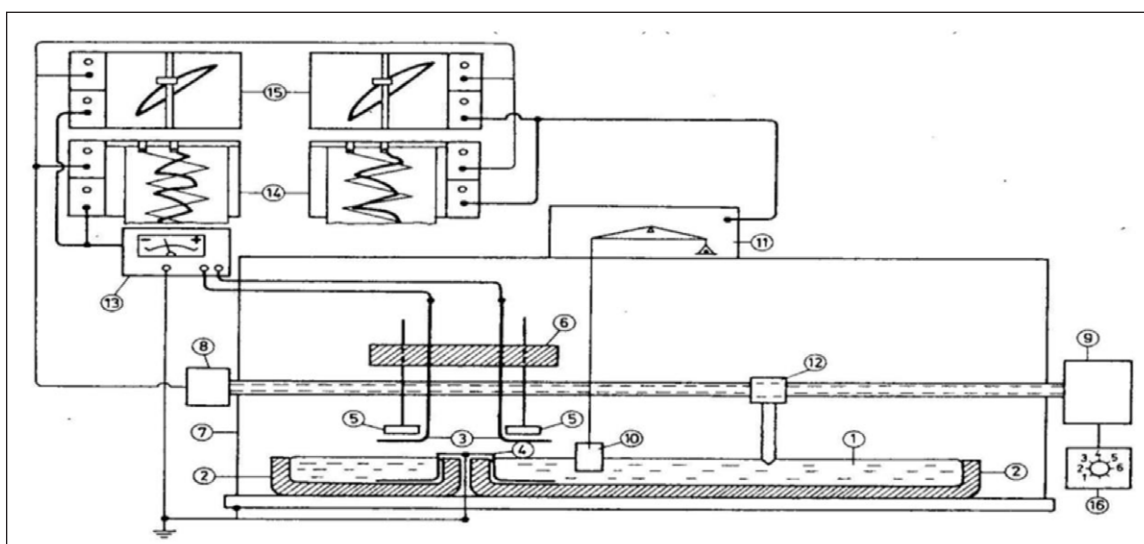


Figure 4: Apparatus for measuring dilation rheology of the surface film together with surface electrical field on the air side. Surface visco-elasticity and surface potential are measured with a Langmuir trough (single oscillating surface PTFE blade, Wilhelmy plate and differential electrometer): 1 – sample trough; 2 – reference trough; 3 - gold-electrode sensors of electrical potential; 4 – electrical ground connection; 5 – radioactive ionization probes; 6 – vertically adjustable electrode holder; 7 – Faraday's cage; 8 – position transducer; 9 – sweep motor and drive; 10 – Wilhelmy-plate surface-tension sensor; 11 – surface tension electrobalance; 12 – PTFE surface sweeper; 13 – differential electrometer; 14 and 15 – recording devices; 16 – sweep-rate controller (Pravdić and Dragčević, 1985). DOI: <https://doi.org/10.1525/elementa.283.f4>

being associated with the elastic response of the material, and the imaginary part G''_{2D} associated with the viscous response. The Lissajous plots of 2D dilation-compression give the modulus $|G^*_{2D}| = \Delta\tau_{2D}/\Delta\gamma_{2D}$ as equal to the slope of the ellipse axis, where $\Delta\gamma_{2D}$ is the total amplitude of variation of γ_{2D} and the viscous modulus G'' is equal to the maximum vertical extent within the ellipse. In this 2D material subject to sinusoidal 2D compression-dilation strain, G^*_{2D} is referred to in the literature as the 2D dilational visco-elastic modulus. It is defined as:

$$G^*_{2D} = -A \frac{d\Delta\tau_{2D}}{dA} = \frac{d\tau_{2D}}{d\gamma_{2D}} \quad (5)$$

The figure traced may be considered a deformed prolate ellipse, with an axis increasing in slope with compression (smaller value of γ_{2D}) and a vertical extent also increasing with compression. This indicates that with increasing compression the surface material became more rigid (high 2D modulus $|G^*_{2D}|$) and more viscous (high value of G''_{2D}).

From Lissajous plots of dynamic surface tension τ_{2D} vs. compression-dilation, 2D rheological properties (2D elastic modulus G'_{2D} and 2D viscous modulus G''_{2D}) can be derived. Lipids and complex surfactant molecules may modify surface properties and bulk-phase rheological properties (Jenkinson and Sun, 2010) more strongly. As the carboxyl (sugar) groups composing carbohydrates are hydrophilic, they will not associate with the water-gas film at molecular scale, but as many carbohydrates are buoyant and associated with TEP (Mari et al., 2016), a fraction of them rise by buoyancy, sometimes aided by incorporated gas bubbles (Wurl et al., 2011), to form a layer of more-or-less broken-up gel just below the film (Wurl and Holmes,

2008). Some of the carbohydrate material is present as functional groups on large molecules that are surfactants *sensu stricto* (Žutić et al., 1981), and such molecules will tend to associate with the surface at polymer-molecule length scale. Buoyancy of TEP is negatively related to pH, so ocean acidification is likely to increase the fraction of TEP associating with the surface film (Mari et al., 2016), and so tend to increase SML rigidity as well as GER.

Analyses of organic matter in the surface layer (Larsson et al., 1974) show concentrations of up to $75 \mu\text{g L}^{-1}$ of saturated and unsaturated ^{16}C and ^{18}C fatty acids. Dragčević et al. (1979) and Dragčević and Pravdić (1981) have discussed whether these fatty acids may or may not form micelles totally or partially reversibly under compression. Such micelle formation, or indeed crumpling of the film downwards into the bulk phase, would absorb energy in separating adsorbed or floating material from the microlayer. At low molecular concentrations in the microlayer, clockwise hysteresis curves of τ_{2D} vs. γ_{2D} (see **Figure 6**) were recorded by Dragčević et al. (1979) and by Van Vleet and Williams (1983), representing positive dissipation of energy; anticlockwise curves were also recorded by Dragčević et al. (1979). The values of this “negative energy” contained in the anticlockwise curves were very small, however, and it is not clear whether they represent measurement artefacts or a real phenomenon. (The phenomenon of “negative energy” in Lissajous curves is addressed by Ewoldt and McKinley, 2009).

The time taken to fully form the mechanical properties of a freshly cleaned sea surface (in the laboratory) were found using surface compression rheometry to be at least 2 h (Dragčević et al., 1979; see their **Figure 5**) for North Adriatic water.

Dragčević et al. (1979) considered that there are three possible processes of surface film formation:

- (1) release of film-forming agent from particulate matter or micelles (aggregates possibly of surfactant matter);
- (2) 2D surface spreading, a process familiar from observing oil slicks; and
- (3) transport from the bulk of the water by diffusion, convection or both to the sea-air surface or to bubbles either in the bulk-water phase or in whitecaps, as well as by mixing and bubble scavenging.

Dragčević et al. (1979) further considered that although the source of the film-forming material is the same for the bubble surfaces and the sea surface, fluid dynamics processes, as well as surface spreading and bubble flotation, may fractionate the various components of the material differently. These authors concluded that the transport and binding of ionic and molecular material at the bubble-water and air-sea interfaces should depend strongly on the properties of the OM in the subsurface layer. Important for modulating gas exchange among these near-surface fluid dynamic processes might be: wind, wave spectra, turbulence from below, surface convergence and divergence, and photosynthetic O₂ production.

The viscous part of the visco-elastic dilational modulus comes from two components: 1) the internal dynamics of the vertical exchanges between the solid, colloidal and dissolved material in the bulk and the surface of the water; and 2) horizontal compression-dilation straining of material closely associated with the surface layer. These exchanges may have many different origins, each process being associated with a characteristic time (Dragčević and Pravdić, 1981). How to separate these two components is still not resolved. Concerning the first component, Pogorzelski and Kogut (2003) concluded from their work on the Baltic and Mediterranean Sea surfaces that, "The stress-relaxation measurements revealed a two-step



Figure 5: Redistribution of surface-associated OM and slick patterns by passage of a ship. Surface wake pattern 100 min after passage of a ship, showing contrast between undisturbed and disturbed surface film patterns. Remastered from Peltzer et al. (1992). DOI: <https://doi.org/10.1525/elementa.283.f5>

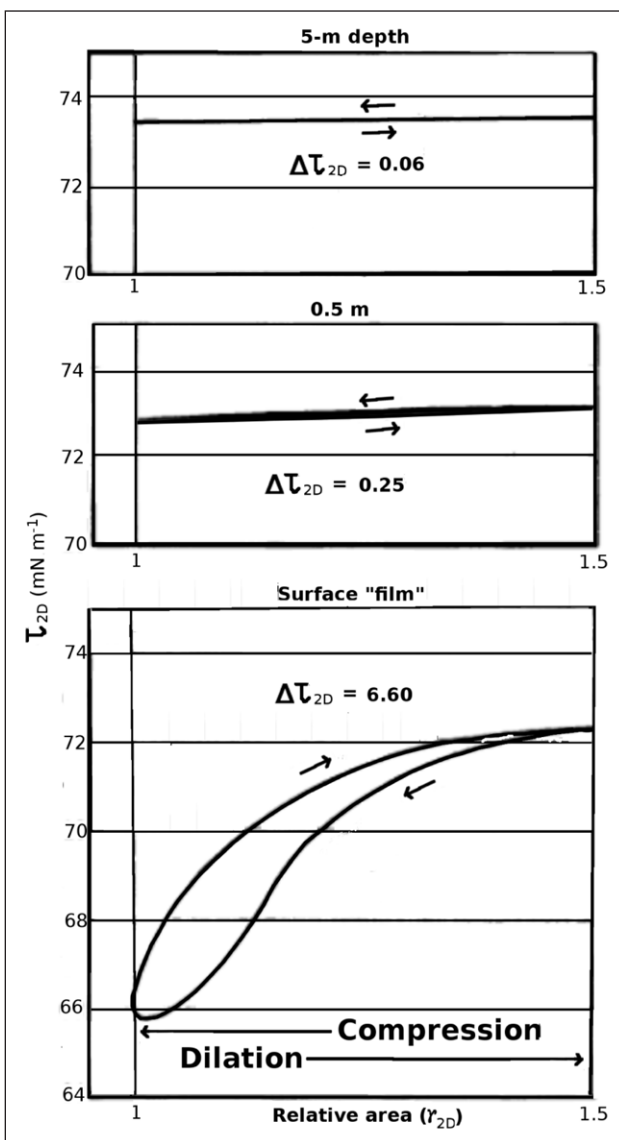


Figure 6: Lissajous plots of measured dynamic surface tension vs. change in surface area. Values of surface tension τ_{2D} vs. γ_{2D} similar to those in Figures 3 and 4. (Redrawn from Dragčević et al., 1979). DOI: <https://doi.org/10.1525/elementa.283.f6>

relaxation process at the interface with characteristic times $t_1 = 1.1-2.8$ and $t_2 = 5.6-25.6$ seconds [which] suggest[s] the presence of diffusion-controlled and structural organisation relaxation phenomena. The[se]... results suggest that natural films are a complex mixture of biomolecules covering a wide range of solubility, surface activity and molecular masses with an apparent structural organisation exhibiting a spatial and temporal variability."

Concerning vertical molecular diffusion Pogorzelski (2001), Pogorzelski and Kogut (2001) and Pogorzelski et al. (2005), reviewing previous work, calculated molecular mass M_w from plots of surface pressure, $\Delta\tau_{2D}$ vs. t for short ($t \rightarrow 0$) and long ($t \rightarrow \infty$) times, and also calculated diffusion coefficient D as if it had been composed of monomers rather than polymeric clusters. Values of M_w scattered widely from 2 to 166 kDa, with a typical value of 50 kDa. The real diffusion rates D_{eff} were mostly lower than D , strongly suggesting that diffusion of the molecules

is hindered by an adsorption barrier crowded with other molecules. Values of D_{eff} were measured, and values of D_{eff}/D presented. In Baltic Sea waters, values of D_{eff}/D in the surface film ranged from 0.16 to 0.01; and in surface films from waters of nearby lakes and rivers, from 0.87 to 0.001. In both the Baltic Sea and in freshwaters, values of D_{eff}/D nearest to unity occurred in February, while the lowest values occurred in May or August, suggesting that reduction in D_{eff} was related to polymers produced by primary production. To account for values of D_{eff}/D far lower than 1, especially in later spring and summer, the authors suggested that the biopolymer molecules must have been aggregated, which concurs with present consensus on the seasonality of primary productivity. Pogorzelski's findings of molecular diffusion reduced relative to calculated diffusion represent evidence that concurs with observations by Sieburth (1983), Wurl and Holmes (2008) and Wurl et al. (2011, 2016), as well as model-aided conclusions of Mari et al. (2016) of more-or-less broken-up gel associated with the surface microlayer. Where foam is present (Section 4), corresponding exchanges take place also between the bulk water, the SML and the foam (Johnson et al., 1989).

3.3.5. 2D shear rheological properties of the surface film

Kuhnenn et al. (2006) carried out measurements of surface shear rheology on the surface of seawater and algal cultures. Measurements were started after the surface film had been removed in order to follow the rate of film formation. The authors reported their results in surface shear viscosity and surface shear rigidity, referring to both the methodology used in a previous study (Krägel et al., 2003) and the website of the apparatus manufacturers (Sinterface Technologies, 2017). However, recovering the surface shear stresses from the data in Kuhnenn et al. (2006) is not possible. The authors reported how surface rheologi-

cal parameters changed over up to 18 h in cultures of the diatoms *Thalassiosira rotula* ($9.8 \times 10^3 \text{ mL}^{-1}$), *T. punctigera* ($11.4 \times 10^3 \text{ mL}^{-1}$) and *Nitzschia closterium* ($2.27 \times 10^6 \text{ mL}^{-1}$), and the haptophyte *Phaeocystis* sp. ($0.12 \times 10^6 \text{ mL}^{-1}$), as well as f/2 culture medium and seawater of salinity 31. Initial values of surface shear viscosity $\eta_{2D,Shear}$ ranged from $2 \mu\text{N s m}^{-1}$ for seawater to 7–8 for *Thalassiosira* and *Phaeocystis* to $12 \mu\text{N s m}^{-1}$ for *Nitzschia*. Over time, $\eta_{2D,Shear}$ for the seawater remained practically unchanged up to 200 min, and it decreased for the other materials except for *Nitzschia*, for which it markedly increased to $33 \mu\text{N s m}^{-1}$ after 610 min before declining slightly. In considering the relatively large surface rheological effects produced in the *Nitzschia closterium* culture, bear in mind firstly that its concentration was much higher in these experiments than those of the *Thalassiosira* species investigated, and that its cell size and carbon content are much larger than *Phaeocystis*, and secondly that in nature *N. closterium*, although frequently found in coastal plankton, associates facultatively with benthic biofilms.

The only other measurements of surface shear rheological properties on the surface film of seawater and phytoplankton cultures appear to have been made by Jenkinson (1993b) to understand interference by surface effects on measurements in the bulk phase, using a Contraves/Mettler LS 40 rheometer and Couette shearing system with a surface bob suspended at the liquid-air interface. Figure 7 (right-hand side) illustrates the measuring system. In this figure, the right-hand insert shows a schematic profile view of a cup and a surface bob for measurements of shear rheology of the air-liquid interface. During measurements, the Couette system was protected from air currents by two Plexiglas boxes, one inside the other. Surface shear stress $\tau_{2D,Shear}$ was found to oscillate with a frequency equal to that of the rotating cup, suggesting more-or-less deformable plaques of material

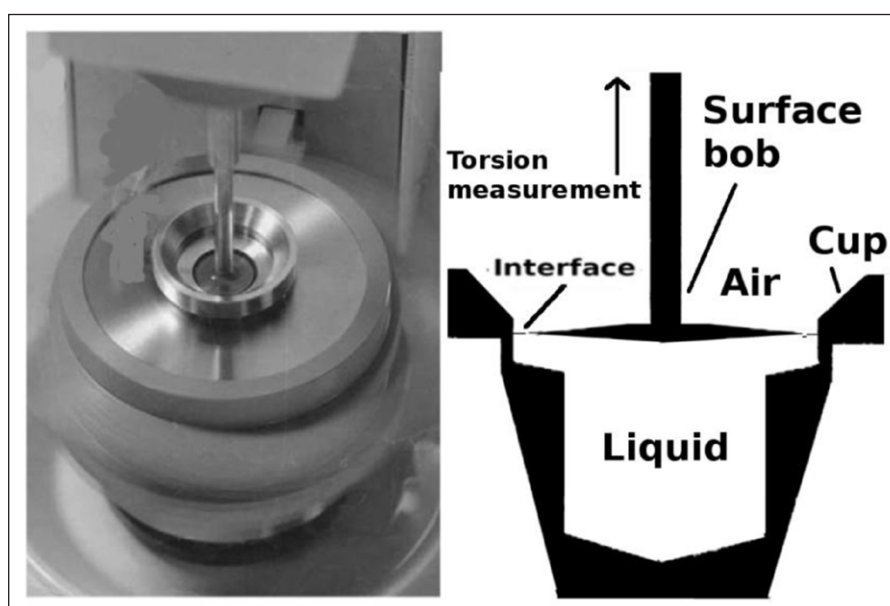


Figure 7: System for measuring 3D bulk-phase shearing rheology and 2D surface-phase shear rheology. Detail of the Contraves/Mettler LOWSHEAR 30 rheometer used by Jenkinson, 1986a, 1993b) and by Jenkinson and Biddanda (1995). Remodelled from manufacturers' promotion literature. DOI: <https://doi.org/10.1525/elementa.283.f7>

at the water-air interface attached to menisci at the cup and the bob, rubbing past each other. Deionized double distilled water that had been kept in a laboratory wash bottle for several days was also measured under continuous rotation for $\tau_{2D, shear}$ on the surface of this water was again found to oscillate with a frequency equal to that of the cup rotation, suggesting a quasi-stable plaque structure formed here as well. For filtered (0.2 μm) seawater the half-amplitude of $\tau_{2D, shear}$ varied from 0.17 mN m^{-1} to 0.34 mN m^{-1} , while a filtered *Skeletonema* culture gave even higher half-amplitude values, up to 2.0 mN m^{-1} . The filtered culture gave $\tau_{2D, shear}$ values that increased quasi-exponentially with time on standing in the cup (Jenkinson, 1993b), reminiscent of the observation by Kuhnenn et al. (2006) for *Nitzschia closterium* culture.

3.3.6. Viscosity of water from the SML measured by fluorescence depolarization

Using fluorescence depolarization (FD), Carlson's team (Carlson, 1987; Carlson et al., 1987) sampled bulk seawater with bottles, and used a glass plate to sample from SMLs, with and without slicks, from eastern and western coastal waters of the USA. For unfiltered samples, unslicked SMLs showed viscosity that was not significantly different from bulk water. In contrast, slicks were significantly more viscous (mean increase of 6%), and filtered (3 μm) slicks were 3% more viscous. Filtered (0.2 μm) unslicked SMLs did not differ from either unslicked SML or bulk water.

Jenkinson and Sun (2010) suggested that a disadvantage of the FD technique was its lack of an association with explicit scales of shear rate or length. It may be possible, however, to calculate length and shear-rate scales from the rotation of the fluorescent molecules (Kuimova et al., 2009), and thus to cross-calibrate them against the specific scales of measurements made with mechanical rheometers.

3.3.7. 3D shear rheology of seawater from the SML

As far as we are aware, the only other rheological measurements comparing the SML with bulk water were made by Jenkinson and Biddanda (1995) in the North Sea during a bloom of *Phaeocystis* sp. and *Noctiluca scintillans* at three stations. The weather was calm and the sea glassy smooth. Rheological measurements were made in a classical low-shear rheometer using a Couette (bob-in-cup) measuring system with the cup rotating back and forth sinusoidally. The mean excess complex (i.e., viscoelastic) modulus was 7 times as high in the SML as in the bulk samples, and the ratio of the elastic modulus to the excess viscous modulus was 52 times as high in the SML as in the bulk samples. Only three SML samples were taken, however, and the differences between the SML and bulk water were not statistically significant.

Zhang et al. (2003a), using capillary flow in an Ubbelohde viscometer, measured viscosity in water from the SML and from underlying water off Jiaozhou Bay, China, in September 2001. Viscosity and DOC values were consistently higher in the SML than in the underlying water, and viscosity in both the SML and the underlying water showed a daily cycle, with highest values between

12h00 and 15h00. DOC values in the SML also showed highest values around this time of day, but any cycle of DOC in the underlying water was less clear.

3.3.8. 3D shear rheology from underlying ocean water

Bulk-phase 3D rheological properties have been measured as a function of phytoplankton taxon. Viscosity and elasticity were measured using Couette geometry (Figure 7, left-hand side) at low shear rates ($<1 \text{ s}^{-1}$). During measurements, the Couette system was protected from air currents by two Plexiglas boxes, one inside the other. Measurements were made of cultures of *Prorocentrum micans*, *Protoperdinium trochoideum*, *Gonyaulax* sp., *Amphidinium* sp., *Dunaliella marina*, *Dunaliella* sp., and a mixed culture of *Noctiluca scintillans* and *D. marina* (Jenkinson, 1986a), and in a culture of *Karenia mikimotoi* (as *Gyrodinium* cf. *aureolum*) and a net-sample from a bloom of *N. scintillans* (Jenkinson, 1993a).

Some species of phytoplankton gave their cultures elasticity and a mostly shear-thinning viscosity in excess of the non-Newtonian viscosity of their culture media. Other species, however, showed no measurable effect. Viscosity η was increased up to 400 times that of the culture medium at a shear rate $\dot{\gamma}$ of 0.002 s^{-1} , which would be typical of the shear rate in much of the ocean below the surface-mixed layer. These results indicate that many species of phytoplankton are able to control the physical properties of the water in which they live, presumably under genetic control and subject to Darwinian-type evolution (Jenkinson and Wyatt, 1995; Wyatt and Ribera d'Alcalà, 2006).

Markedly increased viscosity and even gelling (production of infinite viscosity η at low enough deformation stress τ) has been measured using ichthyoviscometry (flow through gills of dead fish) in cultures of *Karenia mikimotoi* (Jenkinson and Arzul, 1998, 2002) and *Chattonella* spp. (Jenkinson et al., 2007). Viscosity and elasticity have also been measured in oligotrophic Mediterranean water and in a *P. globosa*-dominated bloom in the North Sea (Jenkinson, 1993b; Jenkinson and Biddanda, 1995).

Viscosity measurements in blooms of *Phaeocystis globosa* showed that values of viscosity varied dramatically, in both absolute values and a shift from positive to negative correlation with chlorophyll *a* at a small scale (centimetre to decimetre), as functions of the increase and decline phases of *P. globosa* blooms (Seuront et al., 2007). The authors ascribed the change in correlation sign to motile flagellates leaving the polymer-rich zones with which they were first associated. Foam only occurred during the decline phase.

Seuront et al. (2010), again using a piston-in-cylinder viscometer at sea, found total viscosity η in the Southern Ocean to be increased biologically by up to 85% in subsurface waters, where the increase was associated with bacterial abundance, and up to 78% in the deep chlorophyll maximum, where it was associated with specific phytoplankton taxa.

In freshwater phytoplankton cultures of *Scenedesmus*, *Chlorococcum*, *Porophyridium* and *Spirulina*, viscosity measured by falling ball or rolling ball was in many cases found markedly increased (relative to uninoculated

culture medium (Petkov and Bratkova, 1996). Further details on bulk-phase rheology measurements are reviewed in Jenkinson and Sun (2010) and in Jenkinson et al. (2015). To our knowledge, Seuront et al. (2007) are the only workers who have followed viscosity changes over the course of a bloom *in situ*, and no-one has yet followed such changes in a culture.

With the aim of investigating the effects of length scale on viscosity η , measurements of η were made by Jenkinson and Sun (2014) through capillaries of different diameters. Results showed both increases and decreases of total viscosity (relative to uninoculated culture medium) in cultures of the diatoms *Phaeodactylum tricornutum* and *Skeletonema costatum sensu lato*, the dinoflagellates *Prorocentrum donghaiense*, *Alexandrium catenella* and *Karenia mikimotoi*, as well as of the bacterium *Escherichia coli*. The authors suggested that while the increases were likely caused by thickening due to exopolymeric substances (EPS), the decreases may have been caused by superhydrophobic laminar drag reduction (Rothstein, 2010) at hydrophobic surfaces of either phytoplankton cells or EPS aggregates, or both. Further measurements of this type are needed.

In view of the strongly superhydrophobic surface overlying the SML right at the air-sea interface (van Oss et al., 2005), and its likely importance in modulating fluxes, material from this zone should be carefully investigated for manifestations of superhydrophobic drag reduction during deformation, including rapid movement of the micrometre- to nanometre-thick surface film forced by wind drag.

3.4. Lateral dispersal near the SML

Williams et al. (1986) visually studied lateral and vertical dispersal near the sea surface in light winds and sea states from a small boat using dyes, as a rough function of the measured values of τ_{2D} . We quote from their work directly, to emphasize the details, noting that the symbols have been standardized to the present paper's conventions. "Quantitative measurements of turbulent mixing in the upper 0.1–10 cm of the sea surface were made... under various wind and sea-state conditions. A fine mist of dilute solutions of disodium fluorescein or Rhodamine B or 6G (used as lipid detectors in thin layer chromatography) was sprayed on the sea surface and the rates of spreading and sinking estimated visually. The dye solutions were made using the *in situ* surface water, films collected with the screen, or surface water diluted 5% with distilled water to decrease its density. Dispersion of the dye patch was usually complete (no longer visible) in <5–10s when the surface wave frequencies exceeded 10 cycles per second (onset of gravity waves) and $\Delta\tau_{2D}$ was $<0.5 \text{ N m}^{-1} \times 10^{-3}$."

"When the sea surface was calm (with or without capillary waves) and $\Delta\tau_{2D}$ was about $0.5\text{--}1.5 \text{ N m}^{-1} \times 10^{-3}$, the dye patches persisted up to several minutes before becoming undetectable. When there were obvious films present ($\Delta\tau_{2D} > 1.5 \text{ N m}^{-1} \times 10^{-3}$), then the dispersion times were often greater than 5 but seldom exceeded 10 min."

"A typical measurement went as follows, where $\Delta\tau_{2D} = 1.5\text{--}3 \text{ N m}^{-1} \times 10^{-3}$, windspeed = 5–10 knots, and capillary waves absent: a 20–30 cm diameter dye patch remained intact at the surface for several seconds then slowly spread, forming tendrils which increased in size with time but were still attached to the main patch. After several minutes, the overall diameter of the patch was 2–4 times greater, and it had dispersed vertically to depths of 5–10 cm. Visual disappearance of the patch was complete in 5–10 min" (Williams et al., 1986).

This lengthy passage, quoted almost in full, can be used to gain much insight into possible mechanisms of dispersal in the near-surface layer of the ocean. Even after 5–10 min, the dye patch had dispersed vertically to a depth of only 5–10 cm, even at wind speeds of 5–10 knots (2.7 to 5.4 m s^{-1}). The "tendrils", apparently are part of the dispersion phenomenon, may still need to be explained physically.

3.5. Conclusions about SML physics

Stability or instability of the SML is determined primarily by density due to salt and heat, at least in calm conditions. Additionally, a few nanometres above the SML, between the water surface (with its associated OM) and the air, sits an extremely hydrophobic (non-polar) layer. The dynamics of this layer may be affected by factors such as turbulence in both the air and the water, as well as density stratification and the composition and vertical distribution of hydrophilic, hydrophobic and surfactant molecules in the SML. This layer, repellent to polar molecules, is likely to be crucial in modulating processes such as water-vapour condensation, bubble dynamics and aerosol formation, as well as reducing air-water momentum transfer by electrochemical and nanometre- to micrometre-scale viscosity-reduction mechanisms.

The following possible roles of SML physics in GER need also to be taken into account. Although the role of biologically changed 3D viscosity and 3D elasticity in the underlying water seems unlikely to affect GER directly, some of the OM responsible for this 3D rheological modification exchanges with the SML. In the SML OM also changes both 3D and 2D viscosity and elasticity. 2D rheometry (dynamic surface tension measurements) of water sampled from the surface film and of water sampled from the underlying layer show that 2D viscosity and 2D elasticity in the SML are generally loosely but positively related to primary productivity in the underlying water. Viscosity and elasticity are also generally higher in the SML than in the underlying water. OM released by phytoplankton, and locally by macroalgae, seems to be primarily responsible. GER, increased viscosity, elasticity, algal concentration, bacterial concentration and OM, as well as primary productivity, have been shown to relate positively to each other, albeit with much variance. Rheological modification also depends markedly on both the taxa and the life cycle stage of the organisms present. The strong dependence of 3D and 2D rheological properties on phytoplankton taxa suggests that past and future changes in phytoplankton ecology of the oceans may have a big effect on GER as well as on foam, aerosol and whitecap formation (Section 5), as well as on many fluxes.

Lateral dispersion and concentration of surface-associated OM leads to patterns of slicks easily observed in calm weather. In rough weather, such OM will tend to mix down to a large extent, and any surface patterns that remain would require observation at very small temporal and spatial scales. Recent developments in fluorescence depolarization should also be investigated to discover whether FD can be useful for quick and easy viscosity observations even at sea, and whether it can also incorporate measurements over ranges of length scale.

4. Bubbles, whitecaps, and other foam

4.1. Ecological functions of foams

Foams, including whitecaps and more extensive foam, have ecological functions in oceans, freshwater and salt lakes. For instance, both freshwater and marine foams have been found to efficiently trap particulate organic matter, such as fungal spores (Kohlmeyer, 1984) that can be stored in foams in a viable, ungerminated state for considerable periods of time (Harrington, 1997; Pascoal et al., 2005), dense populations of bacteria, algae and protozoa (Maynard, 1968; Tsyban, 1971; Schlichting, 1974; Velimirov, 1980; Eberlein et al., 1985; Napolitano and Richmond, 1995), and metazoa such as insects, polychaetes, mussels and crustaceans (Castilla et al., 2007). Foams have also been suggested to act as a source of nutrients (Harner et al., 2004) for pelagic and intertidal organisms (Bärlocher et al., 1988; Craig et al., 1989) due to their high calorific content (Velimirov, 1980). Furthermore, ocean foams carrying microbial spores have been proposed as world-wide distribution mechanisms for a variety of organisms (Hamilton and Lenton, 1998). The formation of stable foam near the discharge outlet of effluents from thermal and nuclear power plants is a recent, but growing area of research (Oh et al., 2012). These discharge outlets are particularly favourable to foam formation and persistence, favoured by the higher temperature of the effluent water and air entrainment by pumping, rapid flow and strong local temperature fronts. Such environments may be useful to study for foam dynamics and gas exchange, as physical models of how ocean foaming and gas exchange may react to temperature change.

4.2. Biological aspects of foam formation

Some diatoms (Higgins et al., 2002), dinoflagellates (Honsell et al., 2013; Badylak et al., 2014) and myxobacteria (Wolgemuth et al., 2002), as well as the halophytes *Phaeocystis globosa* and *P. pouchetii*, secrete mucus fibres by exocytosis from pores or nozzles. At least in *Phaeocystis globosa* and *P. pouchetii* cells this mucus consists of mucopolysaccharides, which are stored in secretory vesicles inside the cells in condensed phase (Quesada et al., 2006; Alderkamp et al., 2007). When exocytosed by colonial cells, they rapidly absorb water to become hydrated gels of entangled negatively charged mucopolysaccharides, which form ionic links such as calcium bridges. Within the colony they then form a thin, strong semipermeable colony matrix with pore size between 1 and 4.4 nm in diameter with plastic and elastic properties (Alderkamp et al.,

2007). Matrai et al. (1995) found that, contrary to previous suggestions, these mucopolysaccharides are not available as reserves. When the colony matrices, deserted by their cells, later degrade, these mucopolysaccharides may be released from the colonies as DOM. During this bloom decline phase, the polymeric material may be released from the decaying colonies and may also be degrading, and it may then be apt to form foam. The constituent sugars in carbohydrates secreted by different *Phaeocystis* spp. are reviewed by Alderkamp et al. (2007), who further review the partition into POM and filter-passing DOM. In terms of carbon, POM contributed 10% to 13% in *Phaeocystis* exponential phase, increasing to 38 to 60% in stationary phase, when excess viscosity is highest in blooms (Seuront et al., 2007). However, no data are available for the decline phase, when Seuront et al. (2007) found that most foam occurs. The increase in the proportion of POM as total OM during progression from exponential to stationary phase may indicate increasing polymerisation, which concurs with the increase in viscosity. More details on how the chemical composition, polymeric structure and molecular polarity of this POM and DOM change over the course of *Phaeocystis* blooms, particularly during the decline phase, are required to understand better how these changes affect viscoelasticity, foaming, flotation and other physical effects, especially within the SML. This need for more details applies not only to blooms of *Phaeocystis* spp. but also for phyto- and bacterioplankton more generally.

Furthermore, Biddanda and Benner (1997) found that that the ratio of DOC to TOC during growth of the picocyanobacterium *Synechococcus bacillaris*, the coccolithophorid *Emiliana huxleyi*, the diatom *Skeletonema costatum* and *Phaeocystis* sp. (isolated from the Gulf of Mexico) was 10.8%, 14.1%, 32.4% and 27.0%, respectively, showing that *Phaeocystis* produces plentiful polymeric OM and DOM, but not necessarily more than other phytoplankton; it may be that, rather than being specially abundant, *Phaeocystis* polymers are, relative to their abundance, just powerful precursors of foam.

In the laboratory, Kuhnhen-Dauben et al. (2008) investigated the effects of phytoplankton species, including *Phaeocystis* sp. and *Nitzschia* (= *Cylindrotheca*) *closterium*, and their concentrations, as well as of O₂ and other parameters on bubble residence time t_{bub} after injection of bubbles. t_{bub} correlated only weakly with phytoplankton concentration, except for the case of *N. closterium* where it correlated strongly. t_{bub} also correlated strongly with O₂ concentration and with illumination vs. dark in the presence of phytoplankton (O₂, likely produced by the phytoplankton, added to N₂ already present, increasing total gas partial pressure), but not in experiments in the absence of phytoplankton when O₂ was added from bottles (which may have sparged dissolved N₂ already present, thus changing total gas partial pressure little if at all).

At sea, future investigations of phytoplankton succession should routinely quantify easily observable physical features, such as percentage cover by whitecaps, slicks and foam, to compare with wind speed and wave characteristics.

4.3. Whitecaps – planetary effects

Foams and whitecaps play a major role in modulating global air-sea fluxes that are important to establishing climate at different scales. They also modulate air-sea heat and moisture exchange (Asher et al., 1996; Andreas and Monahan, 2000). In heavy weather, bubble plumes, spray and foams intimately interact in promoting air-sea (Veron, 2015) as well as air-freshwater and -salt lake fluxes. Foams and whitecaps are thus important in establishing global climate. In particular, they are critical in the production of sea-salt aerosols (O'Dowd and de Leeuw, 2007; Booth et al., 2012; Brévière et al., 2015) that contribute to the pool of cloud condensation nuclei in the atmosphere over the ocean, and in bringing to the ocean surface various organic and inorganic surfactant (*sensu stricto*) and sticky materials such as desert Fe-rich dust (Boyd, 2007), soot (Mari et al., 2014) and persistent pollutants (Zhang et al., 2007).

The formation and occurrence of whitecaps have been investigated extensively for the effects of ocean-surface wind vectors (Yueh, 1994) and ocean colour (Gordon and Wang, 1994a, 1994b) on whitecap processes. Blanchard (1985) investigated the roles of whitecaps and bubble bursting on forming sea spray and hence sea-salt aerosols, which modulate the planetary heat budget (Andreas et al., 1995) and ocean-air gas exchange (Asher and Wanninkhof, 1998). Importantly, sea-salt aerosols have the potential to decrease global warming directly by increasing planetary albedo, typically from 0.05 for the ocean to 0.4–0.6 for oceanic foam (Gordon and Jacobs, 1977; Whitlock et al., 1982; Frouin and Murakami, 2007), and indirectly by acting as cloud condensation nuclei (O'Dowd et al., 1999) and by chemically removing methane and surface ozone (Finlayson-Pitts and Pitts, 1997). Sea-salt aerosols may further decrease the cooling effect of sulphate aerosols by rapid removal of anthropic sulphates from the atmosphere and also by preventing the activation of sulphate aerosols as cloud condensation nuclei (Ghan et al., 1998).

Winds stronger than about 5 m s^{-1} produce breaking waves that entrain bubbles down into the mixed layer (Andreas and Monahan, 2000). When such bubbles subsequently rise to the surface, they tend to stick to the TEP, aggregates, phytoplankton and bacteria that they encounter, and so will tend also to bring these types of OM to the surface, sometimes in opposition to ballasting by mineral particles such as diatom frustules and deposited wind-borne dust (Mari et al., 2016), including those in rain or snow (Loÿe-Pilot et al., 1986). The dynamics and rates of bubble-mediated OM rising compared to sinking require quantitative investigation. While the smallest bubbles were found to dissolve fastest in experimentally clean water, POM, by adhering to the bubbles, may slow both their ascent and their dissolution (Detwiler and Blanchard, 1978; Thorpe et al., 1992). In algal blooms bubbles are sometimes produced by increased gas pressure through O_2 production. These bubbles contain gases in proportion to their concentration in the water (not just O_2) and will increase the presentation of these gases, notably N_2 , O_2 and CO_2 , at the surface. Jenkinson and Connors (1980) observed rising by bubbles in a harmful algal

bloom, which has been ascribed to increased polymeric viscosity (Jenkinson, 1986a).

4.4. Whitecap coverage

Monahan and Ó Muircheataigh (1980) plotted data, from one study in freshwater and two on the open ocean, on the coverage fraction by whitecaps. They separated two classes of whitecaps: class A, spilling wave crests and a dense concentration of bubbles; and class B, the diffuse, dissipating remains of class A whitecaps. Based on these data they derived the following relationships. The fraction coverage by class A and class B whitecaps, W_A and W_B , are given in **Equations 5** and **6** (Andreas and Monahan, 2000), while that for total whitecap coverage W_C is given in **Equation 7**.

$$W_A = 3.16 \times 10^{-7} U_{10}^{3.2} \quad (5)$$

$$W_B = 3.84 \times 10^{-6} U_{10}^{3.41} \quad (6)$$

$$W = W_A + W_B \quad (7)$$

where U_{10} is wind speed (m s^{-1}) at a height of 10 m.

Figure 8 shows the data on total whitecap coverage W , compiled by Monahan and Ó Muircheataigh (1980), along with the modelled values (**Equations 5** and **6**) of Andreas and Monahan (2000). Over the range of U_{10} included in these data, 1.6 to 20 m s^{-1} , coverage by type A whitecaps W_A is about an order of magnitude less than that by type B whitecaps W_B . Inspection of the data in this figure shows that for any given value of U_{10} , the range of W is near 10-fold.

Suggestions for this large variation in W have included differences in salinity from freshwater to oceanic, and in temperature, as well as unrecorded differences in wind history, fetch, swell and wave patterns, surface stratification, and surface OM (as “surfactants”). Anguelova and Webster (2006) collated photographic measurements of whitecap coverage W using 853 suitable-quality data points from 28 locations. Measured seawater temperature T_s ranged from -2 to 31°C and measured U_{10} values from 0.1 to 28 m s^{-1} . These data show a strong positive relationship of $\log(W)$ vs. U_{10} and with finite values of W ($\sim 0.01\%$) at U_{10} values as low as $1\text{--}2 \text{ m s}^{-1}$ (**Figure 9a**). The same database showed no clear relationship of W with water temperature T_s or with scatter over three orders of magnitude (**Figure 9b**).

Anguelova and Webster (2006) also compiled data on windspeed U_{10} coverage over the world ocean from satellite observations, and averaged for each latitude-longitude bin over the 31 days of March 1998. From these mean monthly values of U_{10} , they plotted mean values of W modelled using the relationship of Andreas and Monahan (2000) (**Equation 7**; **Figure 10b**). Over the same 31 days, they also plotted mean satellite-observed values of W (**Figure 10a**). The modelled values of W occurred in cold-temperate areas from 40 to 70°S and from 30 to 70°N , with mean modelled W values of $4\text{--}7\%$, compared to W values mostly $<2\%$ in Pacific and Indian Ocean Trade Wind areas. Satellite-observed values of W , however,

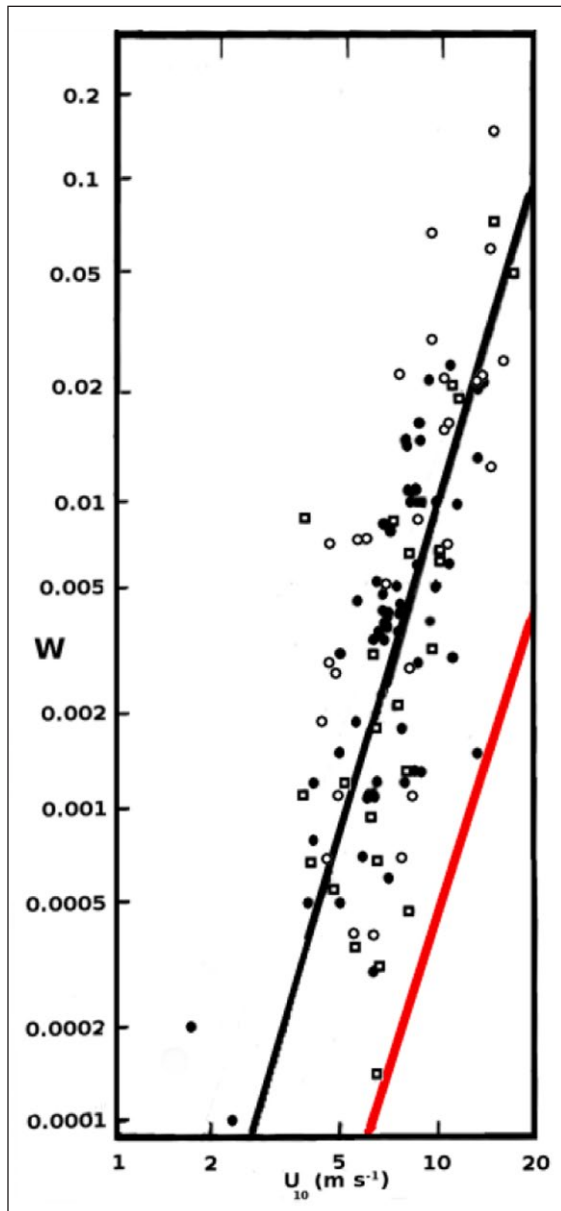


Figure 8: The fraction of the ocean covered by whitecaps versus 10-m elevation wind speed. Filled circles are the white cap fraction W from Monahan (1971); open squares, whitecap fraction from Toba and Chaen (1973); open circles, preliminary whitecap fraction from the 1978 JASIN experiment (Monahan et al., 1983). The red line is W_A (Equation 5) and the black line is W_B (Equation 6). W (Equation 7) is barely distinguishable from W_B on this log-log plot and so is not shown. Data points are taken from Figure 2 of Monahan and Ò Muirheartaigh (1980), and the relationships for W vs. U_{10} are from Andreas and Monahan (2000). DOI: <https://doi.org/10.1525/elementa.283.f8>

showed mean W values mostly $<3.5\%$ in the cold temperate areas but higher than modelled values in the tropical areas of trade winds and ocean gyres, with mean W values mostly $>4.5\%$ in the Pacific Trade Wind area and the Caribbean. The absence of a significant temperature effect on W (Figure 9b) appears to eliminate temperature as an

explanation for relatively greater-than-modelled W values in warm, low-latitude waters than in cold, high-latitude waters. These authors suggested that, as the low-latitude waters are generally more oligotrophic than high-latitude waters, they will have less surface-active material, and that wave-breaking there is less suppressed by “surfactants”, and white-capping enhanced. New work, however, shows that in contrast to previous assumptions, tropical seas tend to be as rich in TEP as temperate seas, perhaps due to the slowness of OM degradation due to nutrient limitation, and also to finding that much TEP is positively buoyant, forms at depth and rises in pulses to surface waters (Mari et al., 2016). Such phenomena could explain why, for equivalent windspeeds, the Trade Wind zones have higher values of W than high-latitude oceans.

Callaghan et al. (2012) photographed whitecap formation and persistence during 551 wave-breaking events at a single location near Martha’s Vineyard, Mass., USA, in October and November 2008. They concluded that the lifetime of whitecaps depends on the bubble persistence time t_{bub} . The authors observed that whitecap decay time ranged 50-fold from 0.2 to 10 s. Particularly as temperature and salinity must have varied little during the observations at the same location, the authors suggested that OM (as “surfactant”) type and quantity may have been a strong element controlling decay time in their study and more generally. Hence the surface coverage of whitecaps is:

$$W = \int_0^{\infty} t_{bub} c_{crest} \Lambda(c_{crest}) dc_{crest} \quad (8)$$

where c_{crest} is the forward speed of the breaking wave crest, and $\Lambda(c_{crest})dc_{crest}$ is the length of breaking crest per area of ocean surface [m^{-2}] observed in the range of speeds $(c_{crest}, c_{crest}+dc_{crest})$. t_{bub} depends on the penetration depth of the bubble plume in the water, and of the presence of “surfactants”.

4.5. Long-lived foaming events

Possible ecological functions of foam are invoked in Section 5.1, and biological mechanisms of foam formation are addressed in Section 5.2. Sometimes, OM produced by phytoplankton is associated with massive foaming and observed foam persistence times of minutes to hours. Such massive foaming occurs at some surface-convergence fronts (Thornton, 1999), where surface-associated particulate, colloidal and dissolved OM accumulates. Other impressive foam events are associated with blooms of the phytoplanktonic halophyte *Phaeocystis globosa* (Figure 11a), and of unknown plankton (Figure 11b), particularly when whipped up by wind and waves on coasts (Jenkinson et al., 2015).

In an integrated study of a *Phaeocystis globosa* bloom, Seuront et al. (2007) showed that over the time scale of the bloom, chlorophyll *a*, excess viscosity and foam presence were intercorrelated. On a finer time scale, however, foam occurred only relatively little while chlorophyll and excess viscosity were increasing, but in large quantities when the bloom was declining, between the

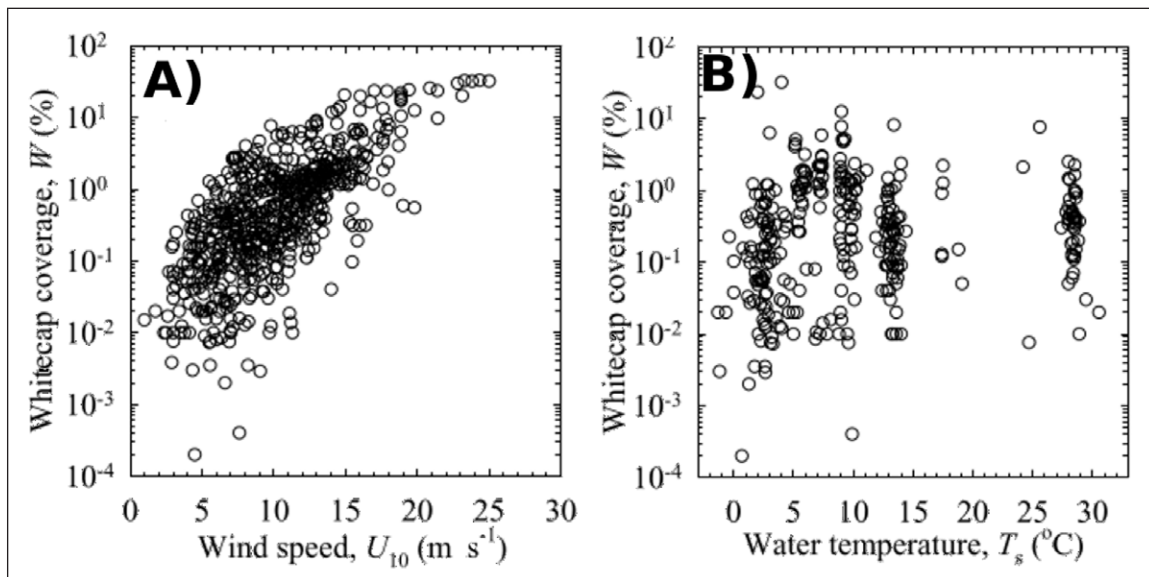


Figure 9: Whitecap coverage vs. 10-m windspeed and sea surface temperature. Photographic measurements of whitecap coverage W (%) at 853 data points from 28 locations. **A)** W vs. wind speed at 10-m elevation (U_{10}); **B)** W vs. sea surface temperature (T_s). Note the large spread in W , as well as the absence of a clear relationship between W and T_s . Redrawn from Anguelova and Webster (2006). DOI: <https://doi.org/10.1525/elementa.283.f9>

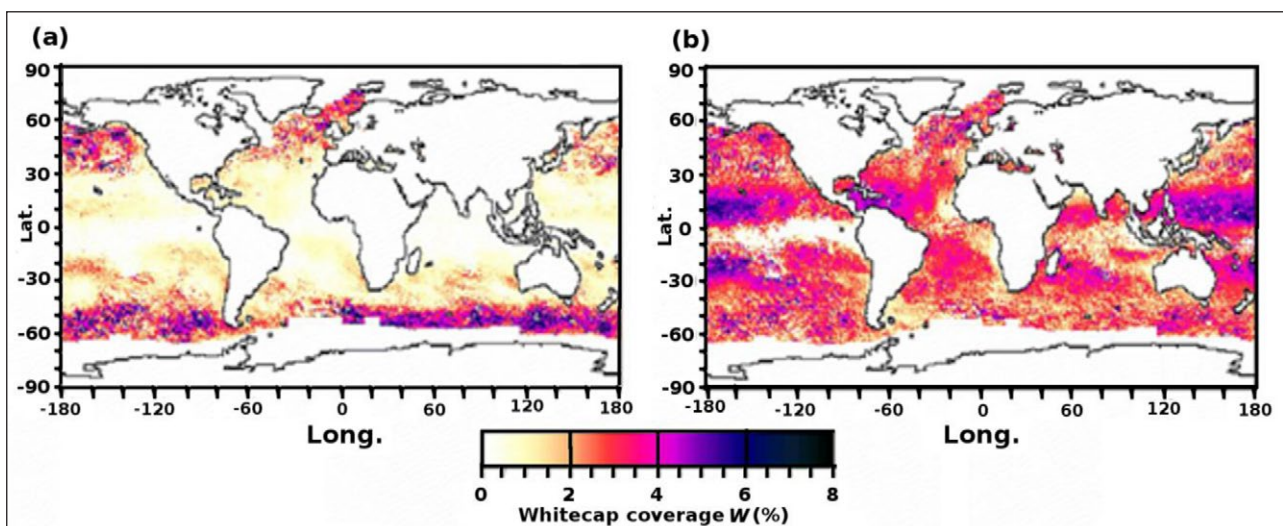


Figure 10: Satellite-photographed whitecap coverage and modelled whitecap coverage. Mean whitecap coverage W for March 1998 (average of 31 daily maps of W). **(a)** Coverage computed with wind speed formula (Equation 7) using daily fields of wind speed; **(b)** Coverage based on satellite measured observations. Redrawn from Anguelova and Webster (2006) with permission from John Wiley and Sons. DOI: <https://doi.org/10.1525/elementa.283.f10>

peak in both chlorophyll and 3D viscosity and the end of the bloom.

Surfactants (*sensu stricto*) stabilize foams and thus tend to increase their lifetime, but small (several micrometres or smaller) hydrophobic solid particles tend to destabilize foams, by mechanisms described in Cantat et al. (2013). Examples of such hydrophobic particles are soot, fine coal dust and some air-borne mineral dusts (Fan et al., 2004). We thus suggest that soot will tend to destabilize ocean foam. In a similar respect, Mari et al. (2014) found that deposition of soot from an oil-fired power station dramatically affected the dynamics of suspended marine

organic aggregates (MOAs), which rapidly increased in size by further aggregation. Mari et al. (2014) invoked this size increase coupled with ballasting by the soot particles (density about 1.8 g cm^{-3}) to explain the rapid sinking of this OM. In turn this sinking of OM could explain its reduction in surface layers, together with decreases in bacteria and viruses, thought by the authors to have been filtered from the water by the sinking MOAs. Thus soot (and black carbon), as well as desert dusts (Pasqueron de Fommervault et al., 2015) may control foam and whitecap production globally by two mechanisms: foam destabilization; and reduction of surface OM concentrations



Figure 11: Massive coastal foam events. a) Foam event at Audresselles, Pas de Calais, France, associated with bloom of *Phaeocystis globosa*. Note the flying foam to the right of the hotel, and also that the hotel roof is partly white, from wind-blown and sticky foam (insert is enlarged to show better some wind-blown foam aggregates); **b)** Foam at Cape Silleiro, Galicia, Spain, about a fortnight after gales in early February 2009. Such foam is produced by the action of breaking waves, entraining air into seawater, itself containing polymeric organic matter produced mainly by phytoplankton. Photos by Laurent Seuront (a) and Tim Wyatt (b). DOI: <https://doi.org/10.1525/elementa.283.f11>

by sticking to and ballasting MOAs, thus producing or increasing their sinking.

4.6. Conclusions about bubbles, whitecaps and other foam

Winds with $U_{10} > \sim 5 \text{ m s}^{-1}$ entrain bubbles into the mixed layer. On rising, these bubbles entrain to the surface TEP, aggregates, phytoplankton and bacteria. When the bubbles burst some of the entrained material is expelled into the atmosphere, where winds disperse a fraction of it. Conversely, some OM, particularly when ballasted by mineral particles, may slow the ascent and dissolution of the smallest bubbles. Particularly in algal blooms during daytime, O_2 production will increase total gas partial pressure, thus driving O_2 and other gases into the atmosphere.

Observations of coverage by whitecaps W in marine and freshwater were made in relation to U_{10} and T_s (where T_s has little effect.) These models were used to predict W around the world ocean. W was predicted to be highest in areas of high U_{10} particularly in the Southern Ocean. Thus these regions were predicted to be of great importance for global fluxes of gases and aerosols. Subsequently, analysis of satellite observations has shown that areas of high W also occur in the trade-wind areas, seriously violating this model, and throwing into doubt ideas on the world distribution of gas exchange, aerosol production and other air-sea fluxes. While the reasons for this discrepancy remain unclear, new findings suggest that tropical seas are richer in TEP than previously thought, and that much of this TEP is positively buoyant, showing pulsed rising to the surface, where TEP and associated OM may stabilise bubbles and whitecaps.

Under certain conditions, more long-lived foam events occur, whose formation is known to be often strongly associated with specific phytoplankton taxa. Foams also play an ecological role in marine and freshwaters by harbouring a variety of organisms, particularly cysts, spores and bacteria, and mediating the injection of such organisms into the atmosphere, where they sometimes disperse widely.

5. Poorly understood factors

5.1. Effects of interaction between rough and very rough weather with the SML

The adsorbed and floating material in the SML influences air-water exchange of gas, water vapour and organic matter itself under both calm and rough conditions. The 2D compression-dilation (CD) surface-film rheology is currently measured using a Langmuir trough and a Wilhelmy plate (Figures 3 and 4), often with simultaneous electrochemical measurements that help reveal the molecular changes during CD (Dragčević et al., 1979; Van Vleet and Williams, 1983). Under rough conditions (Veron, 2015), however, sea-surface phenomena are complex and rapid, so difficult to observe.

5.2. Interactions among parameters

How surfactants *sensu stricto* and other molecules modulate gas exchange across the SML depends on a non-exhaustive list of interacting parameters, including salinity, air and water temperatures, turbulence intensity, wind speed, wave spectra, thermohaline-stratification, the spectrum of incoming and outgoing radiation, rain, snow and dust deposition.

This complexity suggests that full prediction of gas-exchange reduction (GER) from knowledge of the molecular composition of the OM present may be impracticable for the next decade or two, and that empirical measurements of GER for different OM types under different ocean and meteorological conditions may have to be the principal way forward in the short term to understanding how OM and the biological communities that produce it reduce gas exchange in the present and future ocean. This complexity is likely to be increased even further for fluxes during heavy weather (Section 5.1).

5.3. Conclusions about poorly understood factors

Data about rheology of the SML have been obtained mostly in laboratory apparatus at time scales of minutes, and $\dot{\gamma}_{2D} = \sim 0.5$ to 1. Their help in developing models of sea-surface processes must thus be treated with caution even

for calm-sea conditions. Under rough-weather conditions, inspired conceptual models (e.g., Veron, 2015) will be difficult to validate at the suites of scales involved, many of them probably very small. The importance of conceptual models by experienced workers lies in their ability to drive scientific understanding, and the redesign of laboratory apparatus to target different scales of length, time, strain and stress.

Further difficulty in conceiving and validating models of air-ocean fluxes will come from the sheer number of interacting causal factors. Thus, difficulty is likely to remain in validating models, so that the role of empirically obtained data on air-sea-fluxes may need to dominate research on GER and other aspects of air-ocean fluxes for many years to come.

6. Possible responses of SML dynamics and GER to future environmental change

6.1. Possible changes

Any future changes in air-sea exchanges, particularly GER of CO₂ and other substances, are likely to be related in part to changes in the physical and chemical nature of OM produced biologically, largely from phytoplankton-mediated primary production. Here we touch on four current and likely future ocean-wide trends: (1) warming; (2) acidification; (3) increasing eutrophication, with changes in the phytoplankton community and harmful algal blooms; and (4) an increasing or, most likely, decreasing trend in deposition of black carbon.

6.2. Warming

Relative to 1850–1900, global surface temperature over the Earth for 2081–2100 is projected to increase by 1.5°C to over 2°C (IPCC, 2014), with higher than average increases in the Arctic. The heat will take time to penetrate the oceans, so warming here over the same time-frame may be somewhat less, perhaps 1.0 to 1.5°C. The Newtonian viscosity of seawater will decline by about 3% per degree of this temperature increase (Miyake and Koizumi, 1948). However, the effects of temperature on OM contribution to viscosity and elasticity have not yet been investigated for shearing or dilational deformation in water, for either the bulk phase or the SML of the ocean. To our knowledge, rheological and adhesive (surface energy) properties of ocean foams, whitecaps and the air-sea film have similarly not been investigated in relation to environmental change. Therefore, while the Newtonian component of seawater viscosity will decrease by about 3 to 4.5%, we have no data on which to base any predictions of the direct effects of ocean warming on the physical properties of ocean OM.

6.3. Acidification

Relative to 1850–1900, ocean pH has decreased ~0.1 unit, and is projected to decrease by a further 0.06 to 0.3 units by 2081–2100 (IPCC, 2014). To our knowledge, the effect of pH on the physical properties of natural ocean OM has been little investigated (Mari et al., 2017). However, a huge volume of literature exists concerning the effect of pH and other parameters in marine and sewage-sludge

EPS, including divalent ions and salinity, on flocculation and adsorption of OM, particularly in membrane filtration (Baudez et al., 2011; Pilli et al., 2015; Villacorte et al., 2015; Zhang et al., 2016). Some of these studies might be used to inspire work on the effects of pH on flocculation of ocean OM, as well as its adsorption to the hydrophobic air-sea interface, and the effects of such adsorption on gas exchange and foam dynamics. Finally, as mentioned in **Section 4.3.4**, recent work (Mari et al., 2016) has strongly suggested that, in contrast to previous assumptions, much TEP is positively buoyant, representing an upward flux of OM from the deep ocean to the surface, where it may accumulate and provide a reservoir of material associated with the air-surface. Furthermore, TEP buoyancy has been shown to be related negatively to pH (Mari, 2008), so that acidification is likely to increase upward OM flux, with possible increase of OM in the air-sea film, which is associated with reduction of CO₂ exchange (Calleja et al., 2009). If this OM is degraded and respired near the surface, for example as a result of surface nutrient enrichment, the result may be an increase in pCO₂ in surface waters, with a higher net flux of CO₂ from water to air.

6.4. Increasing eutrophication, with changes in the phytoplankton community and harmful algal blooms

Because of increases in nutrient enrichment, largely in coastal waters but also more widely due to dispersal of airborne NO_x from fossil fuel burning, the phytoplankton community is changing and harmful algal blooms are increasing in many parts of the world (Glibert et al., 2012). Many of these blooms form high biomass near the surface, and by allelopathic (Yamasaki et al., 2009) and perhaps mechanical-rheological (Jenkinson and Wyatt 1995; Young et al., 1997) methods damage their predators and competitors, and thereby partly stabilize their own niche (Jenkinson and Wyatt, 1995; Wyatt and Ribera d'Alcalà, 2006). Some species secrete OM that changes visco-elasticity. These species are likely candidates for reinforcement of the air-ocean film, with possible increase in GER. Such biomass will also change partial pressures of dissolved gases, and the export and import fluxes of both CO₂ and fixed C to the water below the SML.

6.5. A decreasing trend in production and deposition of black carbon

Black carbon (BC) is produced by fires. It consists of primary particles typically 10–30 nm diameter that form aggregates of about 50–600 nm equivalent spherical diameter (Bond et al., 2013). Fresh BC is hydrophobic and insoluble in water, although the degree of hydrophobicity declines with aging. Global production of BC is estimated at 8 Tg yr⁻¹, with an uncertainty factor of 2 (Bond et al., 2013).

Some BC enters the coastal ocean in the dissolved (<0.8 μm) form in river runoff, However, most of it enters the global ocean through deposition of airborne, particulate BC (Mari et al., 2017). Airborne BC is part of the family of atmospheric aerosols. While most aerosols contribute net reflexion of radiation from the Earth, BC contributes net absorption. Aerosols as a whole contribute

the largest uncertainty to estimates of total radiative forcing in Earth temperature models (IPCC, 2014). The impact of current climate policy to reduce combustion is predicted to lower production of BC, relative to 2005 levels, by 30% (baseline policy) to 55% (stringent policy) by 2050. As mentioned in **Section 5.2**, small, hydrophobic particles, such as BC, destabilize bubbles and foam, and deposition of BC soot into the ocean surface mixed layer tends to accelerate sinking of marine organic aggregates. This sinking may reduce the pool of OM near the ocean surface and thereby decrease air-ocean film strength and viscosity, reducing GER and increasing gas exchange. How much global impact the present levels of BC deposition have on either destabilizing marine foams including whitecaps, altering OM in the SML, or increasing downward flux of OM is unknown. Research is needed on all of these topics.

6.6. Conclusions about possible responses to future environmental change

The increase in the overall temperature of the oceans predicted for the period 2081–2100, related to that for 1850–1900 will reduce the Newtonian viscosity of seawater by 3–4.5%. However, the effects of this temperature increase on the contribution to viscosity and elasticity by OM, particularly in the SML, and thus on gas exchange appear not to have been investigated.

Recent work suggests the presence of a large body of TEP in deep tropical ocean water that is positively buoyant, and rises up towards the surface in pulses. Moreover, the buoyancy of such TEP has been found negatively related to pH. (Mari, 2008). Future acidification thus might increase this upward OM flux, in turn increasing OM enrichment of the SML (Mari et al., 2016), which would likely tend to increase GER), resulting in lower gas exchange. Furthermore, if some of this OM is degraded near the surface, for example through increasing eutrophication, $p\text{CO}_2$ might increase near the surface, tending to globally reduce ocean sequestration of atmospheric CO_2 .

Because of nutrient enrichment, phytoplankton concentrations, and harmful algal blooms are increasing in many parts of the world. Some of the dominant species secrete OM that markedly increases the viscoelasticity of seawater, making them likely candidates for reinforcement of the air-ocean film, thus further increasing GER. Changes in taxonomic dominance of high-biomass phytoplankton blooms, whether or not associated with climate change, are likely to have sudden and unpredictable changes on GER.

Black carbon is put into the atmosphere mostly by fires. Global policies to reduce combustion and smoke are predicted to decrease BC emissions by 30–55% relative to 2005 levels. Such decrease in BC will tend to increase foam and whitecaps, and accelerate OM sinking thus reducing the pool of OM near the surface. These processes may tend to reduce GER and increase gas exchange. Research is needed on the budget and effects of BC in order to quantify the magnitudes and uncertainties of predicted effects of future BC reduction.

7. General conclusions

In published literature on surfaces between air and natural waters, the terms “surfactant” and “surface active” have been used with various meanings, often loosely defined, and different from those used in organic chemistry and surface science. We have proposed a more precise definition of the term “surfactant”, based on that used in organic chemistry and surface science and that should be easily understood by scientists across disciplines. A surfactant is a substance of which each molecule bears one or more functionally hydrophilic (polar) groups and one or more functionally hydrophobic (non-polar) groups. A further defining property of surfactants is that when they associate with a surface they reduce the surface tension, but other types of molecules can also have this effect.”

Most of the organic matter in the sea-surface microlayer and in the underlying bulk water is derived originally from algal, including cyanobacterial, primary production. A high proportion of this OM is old (days to thousands of years) and biologically refractory, and shows comparatively little rheological, aggregative, adhesive or surface-active behaviour. A smaller fraction of this OM is young (minutes to days), and largely sticky and rheologically active. Some of the young OM is hydrophobic (non-polar), some is hydrophilic (polar) and some is surface-active (i.e., bearing both polar and non-polar radicals).

The surface tension τ_0 of OM-free seawater is about 72.8 mN m^{-1} , depending slightly on temperature and salinity. When the surface film of OM-free water or seawater is subject to cycles of dilation and compression (increase and decrease of surface area) using a “wiper” blade, there is no measured change in the force opposing surface tension τ_{2D} ; i.e., $\Delta\tau_{2D} = 0$. In natural surface films, however, $\Delta\tau_{2D}$ varies as a function of both dilation (elastic force) and of dilation rate (viscous force). Values of $\Delta\tau_{2D}$ have been measured to reach about 7 mN m^{-1} . Deformation against the viscous component of $\Delta\tau_{2D}$ dissipates mechanical energy to heat and hence damps ripples, which are compression-dilation oscillations supported by elasticity, in the surface film. 2D rheological properties of the surface film have furthermore been measured by dilational deformation (dynamic surface tension measurements) and by shearing deformation. Some measurements of shearing forces at the liquid-air film $\tau_{2D, \text{shear}}$ have been measured for seawater, with values of up to 0.17 mN m^{-1} , while values in filtered cultures of the diatom *Skeletonema costatum sensu lato* gave values up to 2.0 mN m^{-1} . Measurements of surface shear viscosity $\eta_{2D, \text{shear}}$ in some other phytoplankton cultures have given values, less than $12 \mu\text{N s m}^{-1}$, much less than for *Skeletonema*.

Viscosity in seawater taken from the SML of slicked and unslicked water has been measured by fluorescence depolarization. Viscosity in unslicked SML was generally higher than in underlying bulk water, and viscosity in slicked SML water even higher.

A large body of data is available on rheologically measured 3D viscosity and elasticity in seawater, including the SML, and in phytoplankton cultures. The 3D viscosity is contributed by a Newtonian component due to water and salts, and a non-Newtonian component due to OM,

probably contributed mostly by young OM. Generally the non-Newtonian component is positively related to phytoplankton concentration, but negatively related to shear rate and to length scale. Viscosity is also related to taxonomic composition of the phytoplankton community present, and to the stage of the bloom cycle. Measurements made on phytoplankton communities in capillary flow (3D shearing) have also shown some viscosity values less than that of phytoplankton in uninoculated culture, medium, which has tentatively been ascribed to superhydrophobic action at sculptured hydrophobic surfaces of cells or organic aggregates, or both.

Whitecap and foam coverage of the ocean surface W show a dominant positive relationship of W to 10-m wind-speed U_{10} , and many other physicochemical parameters also play a role. An important taxon-dependent role is played by phytoplankton blooms. Although much speculation has been published on roles of foam in modulating air-sea fluxes of many properties and substances, including gas, quantitative data is far from sufficient. Worldwide satellite observations have shown that in March W values in trade-wind zones are comparable to those in high latitudes, subject to higher winds and higher primary productivity, thus seriously violating current models of whitecap occurrence. Moreover, recent evidence has been presented of pulses of buoyant TEP migrating upward in tropical oligotrophic zones, which could provide an explanation for this apparent discrepancy. Measurements of CO_2 exchange in different parts of the ocean have recently shown gas exchange reduction of up to about 50% positively related to OM concentration in the top 1 cm of the ocean at U_{10} values $< 5 \text{ m s}^{-1}$.

Resolving the role of biological components in phenomenological models of air-sea exchange of CO_2 , and of other materials and properties, requires co-ordinated studies by interdisciplinary teams with expertise in physical oceanography, meteorology, surface and bulk-phase rheology, as well as phytoplankton physiological ecology and genomics. For windspeeds $U_{10} > \sim 10 \text{ m s}^{-1}$, however, it may be too difficult to resolve the complex small-scale air-sea processes in the foreseeable future, and compilation of global mass-balance budgets may have to be the principal way forward. Even so, it will be an exciting challenge to validate models of how future global changes in temperature, acidity, eutrophication, windspeeds, precipitation and taxon composition will modulate OM-mediated air-sea fluxes, including CO_2 gas exchange reduction.

Acknowledgements

We thank Jody Demers and an anonymous reviewer for greatly improving this paper. We are grateful to Professor Guipeng Yang (Key Laboratory of Marine Chemistry Theory and Technology, Ocean University of China, Qingdao, China) for hosting the SCOR Working Group 141 International Workshop on the Sea Surface Microlayer, as this workshop led to discussions inspiring the present paper. We also thank Zhuo LI (State Key Laboratory of Pollution Control and Resource Reuse, College of Environmental Science and Engineering, Tongji University, Shanghai, China) for important rheological discussions.

Funding information

IRJ thanks the Chinese Society of Oceanology and Limnology and the Chinese Academy of Sciences Institute of Oceanology, Qingdao for continued salary support. Part of this research was financially supported by the Australian Research Council's Discovery Projects funding scheme (Projects DP0664681 and DP0988554 granted to LS). This work is a contribution to the CPER research project CLIMIBIO. We thank the French Ministère de l'Enseignement Supérieur et de la Recherche, the Hauts de France Region and the European Funds for Regional Economical Development for their financial support to this project. HD gratefully acknowledges support from the National Natural Science Foundation of China (No. 41676067), the National Natural Science Foundation for Creative Groups (No. 41521064), and the Fundamental Research Funds for the Central Universities (201762030).

Competing interests

The authors have no competing interests to declare.

Author contributions

- Contributed to conception and design: IRJ, LS, HD, FE
- Contributed to acquisition of data: Not applicable, as this is a review paper
- Contributed to analysis and interpretation of data: IRJ, LS, HD, FE
- Drafted and/or revised the article: IRJ, LS, HD, FE
- Approved the submitted version for publication: IRJ, LS, HD, FE

References

- Adrian, RJ** 2010 Closing in on models of wall turbulence. *Science* **329**: 155–156. DOI: <https://doi.org/10.1126/science.1192013>
- Alderkamp, A-C, Buma, AGJ and van Rijssel, M** 2007 The carbohydrates of *Phaeocystis* and their degradation in the microbial food web. *Biogeochemistry* **83**: 99–118. DOI: <https://doi.org/10.1007/s10533-007-9078-2>
- Alpers, W and Hühnerfuss, H** 1989 The damping of ocean waves by surface films: A new look at an old problem. *J Geophys Res* **94**(C4): 6251–6265. DOI: <https://doi.org/10.1029/JC094iC05p06251>
- Andreas, EL, Edson, IJB, Monahan, EC, Rouault, MR and Smith, SD** 1995 The spray contribution to net evaporation from the sea: a review of recent progress. *Bound-Lay Meteorol* **72**: 3–52. DOI: <https://doi.org/10.1007/bf007123891111>
- Andreas, EL and Monahan, EC** 2000 The role of whitecap bubbles in air-sea heat and moisture exchange. *J Phys Ocean* **30**: 433–442. DOI: [https://doi.org/10.1175/1520-0485\(2000\)030<0433:TROWBI>2.0.CO;2](https://doi.org/10.1175/1520-0485(2000)030<0433:TROWBI>2.0.CO;2)
- Anguelova, MD and Webster, F** 2006 Whitecap coverage from satellite measurements: A first step toward modeling the variability of oceanic whitecaps. *J Geophys Res* **111**(C3): 017. DOI: <https://doi.org/10.1029/2005JC003158>

- Asher, WE, Karle, LM, Higgins, BJ, Farley, PJ, Monahan, EC, et al.** 1996 The influence of bubble plumes on air-seawater gas transfer velocities. *J Geophys Res* **C5**: 12027–12041. DOI: <https://doi.org/10.1029/96JC00121>
- Asher, WE and Wanninkhof, R** 1998 The effect of bubble-mediated gas transfer on purposeful dual gaseous tracer experiments. *J Geophys Res-Oceans* **103**: 10555–10560. DOI: <https://doi.org/10.1029/98JC00245>
- Badylak, S, Philips, EJ, Mathews, AL and Kelley, K** 2014 *Akashiwo sanguinea* (Dinophyceae) extruding mucous from pores on the cell surface *Algae* **29**(3): 197–201. DOI: <https://doi.org/10.4490/algae.2014.29.3.197>
- Bärlocher, F, Gordon, J and Ireland, RJ** 1988 Organic composition of seafoam and its digestion by *Corophium volutator* (Pallas). *J Exp Mar Biol Ecol* **115**: 179–186. DOI: [https://doi.org/10.1016/0022-0981\(88\)90102-5](https://doi.org/10.1016/0022-0981(88)90102-5)
- Barnes, H, Hutton, J and Walters, K** 1989 An introduction to Rheology. Amsterdam, NL: Elsevier.
- Baudez, J, Markis, F, Eshtiaghi, N and Slatter, P** 2011 The anaerobic rheological behaviour of digested sludge. *Water Res* **45**: 5675–5680. DOI: <https://doi.org/10.1016/j.watres.2011.08.035>
- Biddanda, B and Benner, R** 1997 Carbon, nitrogen, and carbohydrate fluxes during the production of particulate and dissolved organic matter by marine phytoplankton. *Limnol Oceanogr* **42**: 506–518. DOI: [https://doi.org/10.1016/0011-7471\(74\)90022-9](https://doi.org/10.1016/0011-7471(74)90022-9)
- Blanchard, DC** 1985 The oceanic production of atmospheric sea salt. *J Geophys Res* **90**: 961–963. DOI: <https://doi.org/10.1029/JC090iC01p00961>
- Bond, TC, Doherty, SJ, Fahey, DW, Forster, PM, Berntsen, T, et al.** 2013 Bounding the role of black carbon in the climate system: A scientific assessment. *J Geophys Res-Atmos* **118**: 5380–5552. DOI: <https://doi.org/10.1002/jgrd.50171>
- Booth, BBB, Dunstone, NJ, Halloran, PR, Andrews, T and Bellouin, N** 2012 Aerosols implicated as a prime driver of twentieth-century North Atlantic climate variability. *Nature* **484**: 228–232. DOI: <https://doi.org/10.1038/nature10946>
- Boyd, P** 2007 Biogeochemistry: iron findings. *Nature* **446**: 989–991. DOI: <https://doi.org/10.1038/446989a>
- Brévière, EHG, Bakker, DCE, Bange, HW, Bates, TS, Bell, TG, et al.** 2015 Surface ocean-lower atmosphere study: scientific synthesis and contribution to Earth system science. *Anthropocene* **12**: 54–68. DOI: <https://doi.org/10.1016/j.ancene.2015.11.001>
- Callaghan, AH, Deane, GB, Stokes, MD and Ward, B** 2012 Observed variation in the decay time of oceanic whitecap foam. *J Geophys Res-Oceans* **117**(C09): 015. DOI: <https://doi.org/10.1029/2012JC008147>
- Calleja, ML, Duarte, CM, Prairie, YT, Agustí, S and Herndl, GJ** 2009 Evidence for surface organic matter modulation of air-sea CO₂ gas exchange. *Biogeosciences* **6**: 1105–1114. DOI: <https://doi.org/10.5194/bg-6-1105-2009>
- Cantat, I, Cohen-Addad, S, Elias, F, Graner, F, Höhler, R, et al. (eds.)** 2013 *Foams*. Oxford, UK: Oxford University Press. DOI: <https://doi.org/10.1093/acprof:oso/9780199662890.001.0001>
- Capone, D, Zehr, J, Paerl, H, Bergman, B and Carpenter, E** 1997 *Trichodesmium*, a globally significant marine cyanobacterium. *Science* **276**: 1221–1229. DOI: <https://doi.org/10.1126/science.276.5316.1221>
- Carlson, DJ** 1987 Viscosity of sea-surface slicks. *Nature* **329**: 823–825. DOI: <https://doi.org/10.1038/329823a0>
- Carlson, DJ, Morril, LE and Brophy, JE** 1987 Techniques of fluorescence depolarization for measuring seawater viscosities. *Limnol Oceanogr* **32**: 1377–1381. DOI: <https://doi.org/10.4319/lo.1987.32.6.1377>
- Castilla, JC, Manriquez, PH, Delgado, AP, Gargallo, L, Leiva, A, et al.** 2007 Bio-foam enhances larval retention in a free-spawning marine tunicate. *P Natl Acad Sci USA* **104**: 18120e–18122e. DOI: <https://doi.org/10.1073/pnas.0708233104>
- Conlisk, AT** 2013 *Essentials of Micro- and Nano-Fluidics*. Cambridge, UK: Cambridge University Press.
- Ćosović, B** 2005 Surface-active properties of the sea surface microlayer and consequences for pollution in the Mediterranean Sea. In: Saliot, A (ed.), *The Mediterranean Sea* **5**: 269–296. Handbook of Environmental Chemistry. Berlin: Springer-Verlag. DOI: <https://doi.org/10.1007/b107150>
- Craig, D, Ireland, RJ and Bärlocher, F** 1989 Seasonal variation in the organic composition of seafoam. *J Exp Mar Biol Ecol* **130**: 71–80. DOI: [https://doi.org/10.1016/0022-0981\(89\)90019-1](https://doi.org/10.1016/0022-0981(89)90019-1)
- Cunliffe, M, Engel, A, Frka, S, Gašparovic, B, Guitart, C, et al.** 2013 Sea surface microlayers: a unified physicochemical and biological perspective of the air-ocean interface. *Progr Oceanogr* **109**: 104–116. DOI: <https://doi.org/10.1016/j.pocean.2012.08.004>
- Deacon, E** 1979 The role of coral mucus in reducing the wind drag over coral reefs. *Bound-Lay Meteorol* **17**: 517–521. DOI: <https://doi.org/10.1111/j.2153-3490.1977.tb00746.x>
- Detwiler, A and Blanchard, DC** 1978 Aging and bursting bubbles in trace-contaminated water. *Chem Eng Sci* **33**: 9–13. DOI: [https://doi.org/10.1016/0009-2509\(78\)85061-1](https://doi.org/10.1016/0009-2509(78)85061-1)
- Dragčević, D and Pravdić, V** 1980 Steady-state relaxation times of surfactant films at the water/air interface. *Croat Chem Acta* **53**: 1–7.
- Dragčević, D and Pravdić, V** 1981 Properties of the seawater-air interface 2. Rates of surface film formation under steady-state oscillations. *Limnol Oceanogr* **26**: 492–495. DOI: <https://doi.org/10.4319/lo.1981.26.3.0492>
- Dragčević, D, Vuković, M, Čukman, D and Pravdić, V** 1979 Properties of the seawater-air interface. Dynamic surface tension studies. *Limnol Oceanogr*

- 24: 1022–1030. DOI: <https://doi.org/10.4319/lo.1979.24.6.1022>
- Eberlein, K, Leal, MT, Hammer, KD and Hickel, W** 1985 Dissolved organic substances during a *Phaeocystis pouchetii* bloom in the German Bight (North Sea). *Mar Biol* **89**: 311–316. DOI: <https://doi.org/10.1007/BF00393665>
- Engel, A, Bange, HW, Cunliffe, M, Burrows, SM, Friedrichs, G, et al.** 2017b The ocean's vital skin: toward an integrated understanding of the sea surface microlayer. *Front Mar Sci* **4**: 165. DOI: <https://doi.org/10.3389/fmars.2017.00165>
- Engel, A, Piontek, J, Metfies, K, Endres, S, Sprong, P, et al.** 2017a Inter-annual variability of transparent exopolymer particles in the Arctic Ocean reveals high sensitivity to ecosystem changes. *Sci Rep-UK* **7**: 4129. DOI: <https://doi.org/10.1038/s41598-017-04106-9>
- Ewoldt, RH and McKinley, GH** 2009 On secondary loops in LAOS via self-intersection of Lissajous-Bowditch curves. *Rheol Acta* **49**: 213–219. DOI: <https://doi.org/10.1007/s00397-009-0408-2>
- Fan, SM, Horowitz, LW, Levy, H and Moxim, WJ** 2004 Impact of air pollution on wet deposition of mineral dust aerosols. *Geophys Res Lett* **31**(L02): 104. DOI: <https://doi.org/10.1029/2003GL018501>
- Finlayson-Pitts, BJ and Pitts, JN** 1997 Tropospheric air pollution: ozone, airborne toxics, polycyclic aromatic hydrocarbons, and particles. *Science* **276**: 1045–1052. DOI: <https://doi.org/10.1126/science.276.5315.1045>
- Franklin, B, Brownrigg, W and Farish, R** 1774 Of the stilling of waves by means of oil. *Philos T Roy Soc Lond* **64**: 445–460. DOI: <https://doi.org/10.1098/rstl.1774.0044>
- Frew, NM, Goldman, JC, Dennett, MR and Johnson, AS** 1990 Impact of phytoplankton-generated surfactants on air-sea gas exchange. *J Geophys Res* **95**: 3337–3352. DOI: <https://doi.org/10.1029/JC095iC03p03337>
- Frew, NM and Nelson, RK** 1992a Isolation of marine microlayer film surfactants for ex situ study of their surface physical and chemical properties. *J Geophys Res-Oceans* **97**(C4): 5281–5290. DOI: <https://doi.org/10.1029/91JC02724>
- Frew, NM and Nelson, RK** 1992b Scaling of marine microlayer film surface pressure-area isotherms using chemical attributes. *J Geophys Res-Oceans* **97**(C4): 5291–5300. DOI: <https://doi.org/10.1029/91JC02723>
- Frew, NM, Nelson, RK and Johnson, CG** 2006 Sea slicks: variability in chemical composition and surface elasticity. In: Gade, M, Hühnerfuss, H and Korenowski, G (eds.), *Marine Surface Films*, 45–56. Berlin: Springer.
- Friedlingstein, P, Andrew, RM, Rogelj, J, Peters, GP, Canadell, JG, et al.** 2014 Persistent growth of CO₂ emissions and implications for reaching climate targets. *Nature Geoscience* **7**: 709–715. DOI: <https://doi.org/10.1038/ngeo2248>
- Frouin, R and Murakami, H** 2007 Estimating photo-synthetically available radiation at the ocean surface from ADEOS-II global imager data. *J Oceanogr* **63**: 493–503. DOI: <https://doi.org/10.1007/s10872-007-0044-3>
- Ghan, SJ, Guzman, G and Abdul-Razzak, H** 1998 Competition between sea salt and sulfate particles as cloud condensation nuclei. *J Atmos Sci* **55**: 3340–3347. DOI: [https://doi.org/10.1175/1520-0469\(1998\)055<3340:CBSSAS>2.0.CO;2](https://doi.org/10.1175/1520-0469(1998)055<3340:CBSSAS>2.0.CO;2)
- Giussani, V, Sbrana, F, Asnaghi, V, Vassalli, M, Faimali, M, et al.** 2015 Active role of the mucilage in the toxicity mechanism of the harmful benthic dinoflagellate. *Ostreopsis cf. ovata. Harmful Algae* **44**: 46–53. DOI: <https://doi.org/10.1016/j.hal.2015.02.006>
- Glibert, PM, Anderson, DM, Gentien, P, Granéli, E and Sellner, KG** 2005 The global, complex phenomena of harmful algal blooms. *Oceanography* **18**: 136–147. DOI: <https://doi.org/10.5670/oceanog.2005.49>
- Glibert, PM, Burkholder, JM and Kana, TM** 2012 Recent insights about relationships between nutrient availability, forms, and stoichiometry, and the distribution, ecophysiology, and food web effects of pelagic and benthic *Prorocentrum* species. *Harmful Algae* **14**: 231–259. DOI: <https://doi.org/10.1016/j.hal.2011.10.023>
- Goldman, JC, Dennett, MR and Frew, NM** 1988 Surfactant effects on air-sea gas exchange under turbulent conditions. *Deep Sea Res Part A* **35**: 1953–1970. DOI: [https://doi.org/10.1016/0198-0149\(88\)90119-7](https://doi.org/10.1016/0198-0149(88)90119-7)
- Gordon, HR and Jacobs, MM** 1977 Albedo of the ocean-atmosphere system: influence of sea foam. *Appl Optics* **16**: 2275–2260. DOI: <https://doi.org/10.1364/AO.16.002257>
- Gordon, HR and Wang, M** 1994a Retrieval of water-leaving radiance and aerosol optical thickness over the oceans with SeaWiFS: a preliminary algorithm. *Appl Optics* **33**: 443–452. DOI: <https://doi.org/10.1364/AO.33.000443>
- Gordon, HR and Wang, M** 1994b Influence of oceanic whitecaps on atmospheric correction of ocean-color sensors. *Appl Optics* **33**: 7754–7763. DOI: <https://doi.org/10.1364/AO.33.007754>
- Hamilton, W and Lenton, T** 1998 Spora and Gaia: how microbes fly with their clouds. *Ethol Ecol Evol* **10**: 1–16. DOI: <https://doi.org/10.1080/08927014.1998.9522867>
- Hansell, DA, Carlson, CA, Repeta, DJ and Schlitzer, R** 2009 Dissolved organic matter in the ocean: a controversy stimulates new insights. *Oceanography* **22**(4): 202–211. DOI: <https://doi.org/10.5670/oceanog.2009.109>
- Harner, MJ, Ramsey, PW and Rillig, MC** 2004 Protein accumulation and distribution in floodplain soils and river foam. *Ecol Lett* **7**: 829–836. DOI: <https://doi.org/10.1111/j.1461-0248.2004.00638.x>
- Harrington, TJ** 1997 Aquatic hyphomycetes of 21 rivers in southern Ireland. *P Roy Ir Acad* **97B**: 139–148.

- Higgins, MJ, Crawford, SA, Mulvaney, P and Wetherbee, R** 2002 Characterization of the adhesive mucilages secreted by live diatom cells using atomic force microscopy. *Protist* **153**: 25–38. DOI: <https://doi.org/10.1078/1434-4610-00080>
- Honsell, G, Bonifacio, A, Bortoli, MD, Penna, A, Battocchi, C, et al.** 2013 New Insights on cytological and metabolic features of *Ostreopsis cf. ovata* Fukuyo (Dinophyceae): A multidisciplinary approach. *PLoS ONE* **8**: e57291. DOI: <https://doi.org/10.1371/journal.pone.0057291>
- Hühnerfuss, H** 2006 Oil on troubled waters – a historical survey. In: Gade, M, Korenowski, CG and Hühnerfuss, H (eds.), *Marine Surface Films*, 3–12. Berlin: Springer. DOI: https://doi.org/10.1007/3-540-33271-5_1
- IPCC – International Panel on Climate Change (Field CB, Barros, VR, et al. (eds.)** 2014 *Climate Change 2014: Impacts, Adaptation, and Vulnerability. Part A*. Cambridge, UK: Cambridge University Press.
- Jarvis, N, Garrett, W, Scheiman, M and Timmons, C** 1967 Surface chemical characterization of surface-active material in seawater. *Limnol Oceanogr* **12**: 88–96. DOI: <https://doi.org/10.4319/lo.1967.12.1.0088>
- Jenkinson, IR** 1986a Oceanographic implications of non-newtonian properties found in phytoplankton cultures. *Nature* **323**: 435–437. DOI: <https://doi.org/10.1038/323435a0>
- Jenkinson, IR** 1986b *Halosphaera viridis*, *Ditylum brightwellii* and other phytoplankton in the north-eastern North Atlantic in spring: Sinking, rising and relative abundance. *Ophelia* **26**: 233–253. DOI: <https://doi.org/10.1080/00785326.1986.10421991>
- Jenkinson, IR** 1993a Viscosity and elasticity of *Gyrodinium cf. aureolum* and *Noctiluca scintillans* exudates in relation to mortality of fish and damping of turbulence. In: Smayda, T and Shimizu, Y (eds.), *Toxic Phytoplankton Blooms in the Sea*, 757–762. Amsterdam: Elsevier.
- Jenkinson, IR** 1993b Bulk-phase viscoelastic properties of seawater. *Oceanologica Acta* **16**: 317–334.
- Jenkinson, IR** 2014 Nano- and microfluidics, rheology, exopolymeric substances and fluid dynamics in calanoid copepods. In: Seuront, L (ed.), *Copepods: Diversity, Habitat and Behavior*, 181–214. New York: Nova Science Publishers.
- Jenkinson, IR and Arzul, G** 1998 Effect of the flagellates, *Gymnodinium mikimotoi*, *Heterosigma akashiwo*, and *Pavlova lutheri*, on flow through fish gills. In: Reguera, B, Blanco, J, Fernandez, M and Wyatt, T (eds.), *Harmful Algae*, Pontevedra, 425–428. Spain and Paris: Xunta de Galicia and IOC of Unesco.
- Jenkinson, IR and Arzul, G** 2002 Mitigation by cysteine compounds of rheotoxicity, cytotoxicity and fish mortality caused by the dinoflagellates, *Gymnodinium mikimotoi* and *G.cf. maguelonnense*. In: Hallegraeff, G, Blackburn, S, Bolch, C and Lewis, R (eds.), *Harmful Algal Blooms 2000*, 461–464. Paris: IOC of UNESCO.
- Jenkinson, IR and Biddanda, BA** 1995 Bulk-phase viscoelastic properties of seawater: relationship with plankton components. *J Plankton Res* **17**: 2251–2274. DOI: <https://doi.org/10.1093/plankt/17.12.2251>
- Jenkinson, IR and Connors, PP** 1980 The occurrence of the red-tide organism, *Gyrodinium aureolum* Hulburt (Dinophyceae) around the south and west of Ireland in August and September, 1979. *J Sherkin Isl* **1**(1): 127–146.
- Jenkinson, IR, Shikata, T and Honjo, T** 2007 Modified ichthyoviscometer shows high viscosity in *Chattonella* culture. *Harmful Algae News* **35**: 1–5.
- Jenkinson, IR and Sun, J** 2010 Rheological properties of natural waters with regard to plankton thin layers. A short review. *J Mar Syst* **83**: 287–297. DOI: <https://doi.org/10.1016/j.jmarsys.2010.04.004>
- Jenkinson, IR and Sun, J** 2014 Drag increase and drag reduction found in phytoplankton and bacterial cultures in laminar flow: Are cell surfaces and EPS producing rheological thickening and a Lotus-Leaf Effect? *Deep Sea Res II* **101**: 216–230. DOI: <https://doi.org/10.1016/j.dsr2.2013.05.028>
- Jenkinson, IR, Sun, XX and Seuront, L** 2015 Thalassorheology, organic matter and plankton: towards a more viscous approach in plankton ecology. *J Plankton Res* **37**(6): 1100–1109. DOI: <https://doi.org/10.1093/plankt/fbv071>
- Jenkinson, IR and Wyatt, T** 1995 Management by phytoplankton of physical oceanographic parameters. Does bloom phytoplankton manage the physical oceanographic environment? In: Lassus, P, Arzul, G, Erard, E, Gentien, P and Marcaillou, C (eds.), *Harmful Marine Algal Blooms*, 603–607. Paris: Lavoisier Intercept.
- Johnson, BD, Zhou, X, Parrish, CC, Wangersky, PJ and Kerman, BR** 1989 Fractionation of particulate matter, the trace metals Cu, Cd, and Zn, and lipids in foam and water below Niagara Falls. *J Great Lakes Res* **15**: 189–196. DOI: [https://doi.org/10.1016/S0380-1330\(89\)71474-X](https://doi.org/10.1016/S0380-1330(89)71474-X)
- Kohlmeyer, J** 1984 Tropical marine fungi. *PSZNI Mar Ecol* **5**: 239–378. DOI: <https://doi.org/10.1111/j.1439-0485.1984.tb00130.x>
- Krägel, J, O'Neill, M, Makievski, A, Michel, M, Leser, M and Miller, R** 2003 Dynamics of mixed protein-surfactant layers adsorbed at the water/air and water/oil interface. *Coll Surf B: Biointerfaces* **31**: 107–114. DOI: [https://doi.org/10.1016/S0927-7765\(03\)00047-X](https://doi.org/10.1016/S0927-7765(03)00047-X)
- Kuhnenn, V, Krägel, J, Horstmann, U and Miller, R** 2006 Surface shear rheological studies of marine phytoplankton cultures – *Nitzschia closterium*, *Thalassiosira rotula*, *Thalassiosira punctigera* and *Phaeocystis* sp. *Colloids Surf B Biointerfaces* **47**: 29–35. DOI: <https://doi.org/10.1016/j.colsurfb.2005.11.021>
- Kuhnenn-Dauben, V, Purdie, DA, Knispel, U, Voss, H and Horstmann, U** 2008 Effect of phytoplankton growth on air bubble residence time in seawater. *J Geophys Res* **113**(C6): 009. DOI: <https://doi.org/10.1029/2007JC004232>

- Kuimova, MK, Botchway, SW, Parker, AW, Balaz, M, Collins, HA, et al.** 2009 Imaging intracellular viscosity of a single cell during photoinduced cell death. *Nature Chem* **1**: 69–73. DOI: <https://doi.org/10.1038/nchem.120>
- Larsson, K, Odham, G and Södergren, A** 1974 On lipid surface films on the sea. I. A simple method for sampling and studies of composition. *Mar Chem* **2**: 49–57. DOI: [https://doi.org/10.1016/0304-4203\(74\)90005-X](https://doi.org/10.1016/0304-4203(74)90005-X)
- Lassus, P, Chomérat, N, Hess, P and Nézan, E** 2016 *Toxic and Harmful Microalgae of the World Ocean*. Copenhagen and Paris: International Society for the Study of Harmful Algae and IOC of UNESCO. *IOC Manuals and Guides* **68**.
- Le Quéré, C, Moriarty, R, Andrew, RM, Peters, GP, Ciais, P, et al.** 2015 Global carbon budget 2014. *Earth System Science Data* **7**: 47–85. DOI: <https://doi.org/10.5194/essdd-7-521-2014>
- Liss, PS and Slater, PG** 1974 Flux of gases across the air-sea interface. *Nature* **247**: 181–184. DOI: <https://doi.org/10.1038/247181a0>
- Loje-Pilot, MD, Martin, JM and Morelli, J** 1986 Influence of Saharan dust on the rain acidity and atmospheric input to the Mediterranean. *Nature* **321**: 427–428. DOI: <https://doi.org/10.1038/321427a0>
- Lucassen-Reynders, E and Lucassen, J** 1970 Properties of capillary waves. *Adv Coll Interf Sci* **2**: 347–395. DOI: [https://doi.org/10.1016/0001-8686\(70\)80001-X](https://doi.org/10.1016/0001-8686(70)80001-X)
- Mari, X** 2008 Does ocean acidification induce an upward flux of marine aggregates? *Biogeosciences* **5**: 1023–1031. DOI: <https://doi.org/10.5194/bg-5-1023-2008>
- Mari, X, Lefèvre, J, Torrétón, J-P, Bettarel, Y, Pringault, O, et al.** 2014 Effects of soot deposition on particle dynamics and microbial processes in marine surface waters *Global Biogeochem Sci* **28**: 662–678. DOI: <https://doi.org/10.1002/2014GB004878>
- Mari, X, Passow, U, Migon, C, Burd, AB and Legendre, L** 2016 Transparent exopolymer particles: Effects on carbon cycling in the ocean. *Progr Oceanogr* **151**: 13–37. DOI: <https://doi.org/10.1016/j.pocan.2016.11.002>
- Mari, X, Van, TC, Guinot, B, Brune, J, Lefebvre, J-P, et al.** 2017 Seasonal dynamics of atmospheric and river inputs of black carbon, and impacts on biogeochemical cycles in Halong Bay, Vietnam. *Elem Sci Anth* **5**: 75. DOI: <https://doi.org/10.1525/elementa.255>
- Matrai, PA, Vernet, M, Hood, R, Jennings, A, Brody, E, et al.** 1995 Light-dependence of carbon and sulfur production by polar clones of the genus. *Phaeocystis*. *Mar Biol* **124**: 157–167. DOI: <https://doi.org/10.1007/BF00349157>
- Maynard, NG** 1968 Aquatic foams as an ecological habitat. *Z f allgem Mikrobiologie* **8**: 119–126. DOI: <https://doi.org/10.1002/jobm.3630080205>
- Miyake, Y and Koizumi, M** 1948 The measurement of the viscosity coefficients of seawater. *J Mar Res* **7**: 63–66.
- Monahan, EC** 1971 Oceanic whitecaps. *J Phys Oceanogr* **1**: 139–144. DOI: [https://doi.org/10.1175/1520-0485\(1971\)001<0139:OW>2.0.CO;2](https://doi.org/10.1175/1520-0485(1971)001<0139:OW>2.0.CO;2)
- Monahan, EC, Fairall, CW, Davidson, KL and Boyle, PJ** 1983 Observed inter-relations between 10m winds, ocean whitecaps and marine aerosols. *Quart J Roy met Soc* **109**: 379–392. DOI: <https://doi.org/10.1002/qj.49710946010>
- Monahan, EC and Muircheartaigh, I** 1980 Optimal power-law description of oceanic whitecap coverage dependence on wind speed. *J Phys Oceanogr* **10**: 2094–2099. DOI: [https://doi.org/10.1175/1520-0485\(1980\)010<2094:OPLDOO>2.0.CO;2](https://doi.org/10.1175/1520-0485(1980)010<2094:OPLDOO>2.0.CO;2)
- Napolitano, GE and Richmond, JE** 1995 Enrichment of biogenic lipids, hydrocarbons and PCBs in stream-surface foams. *Env Toxicol Chem* **14**: 197–201. DOI: <https://doi.org/10.1002/etc.5620140203>
- Nebbioso, A and Piccolo, A** 2013 Molecular characterization of dissolved organic matter (DOM): A critical review. *Anal Bioanal Chem* **405**: 109–124. DOI: <https://doi.org/10.1007/s00216-012-6363-2>
- O'Dowd, CD and de Leeuw, G** 2007 Marine aerosol production: A review of the current knowledge. *Phil Trans Roy Soc Lond A* **367**: 1753–1774. DOI: <https://doi.org/10.1098/rsta.2007.2043>
- O'Dowd, CD, Lowe, JA, Smith, MH and Kaye, AD** 1999 The relative importance of non-sea-salt sulphate and sea-salt aerosol to the marine cloud condensation nuclei population: An improved multi-component aerosol-cloud droplet parametrization. *Quart J Roy Met Soc* **125**: 1295–1313. DOI: <https://doi.org/10.1002/qj.1999.49712555610>
- Oh, S-H, Oh, YM, Kim, J-Y and Kang, K-S** 2012 A case study on the design of condenser effluent outlet of thermal power plant to reduce foam emitted to surrounding seacoast. *Ocean Eng* **47**: 59–64. DOI: <https://doi.org/10.1016/j.oceaneng.2012.03.009>
- Orr, JC, Fabry, V, Aumont, O, Bopp, L, Doney, et al.** 2005 Anthropogenic ocean acidification over the twenty-first century and its impact on calcifying organisms. *Nature* **437**: 681–686. DOI: <https://doi.org/10.1038/nature04095>
- Pascoal, C, Marvanová, L and Cássio, F** 2005 Aquatic hyphomycete diversity in streams of Northwest Portugal. *Fungal Diversity* **19**: 109–128.
- Pasqueron de Fommervault, O, D'Ortenzio, F, Mangin, A, Serra, R, Migon, C, et al.** 2015 Seasonal variability of nutrient concentrations in the Mediterranean Sea: contribution of Bio-Argo floats. *J Geophys Res Oceans* **120**: 8528–8550. DOI: <https://doi.org/10.1002/2015JC011103>
- Patrício, P, Almeida, PL, Portela, R, Sobral, RG, Grilo, IR, et al.** 2015 Living bacteria rheology: population growth, aggregation patterns, and collective behavior under different shear flows. *Phys Rev E* **90**: 0227720. DOI: <https://doi.org/10.1103/PhysRevE.90.022720>

- Peltzer, RD, Griffin, OM, Barger, WR and Kaiser, JAC** 1992 High-resolution measurement of surface-active film redistribution in ship wakes. *J Geophys Res* **97**(C4): 5231–5252. DOI: <https://doi.org/10.1029/91JC01875>
- Petkov, GD and Bratkova, SG** 1996 Viscosity of algal cultures and estimation of turbulence to devices for the mass culture of microalgae. *ArchfHydrobiologie Supplement on Algological studies* **114**: 99–104.
- Pilli, S, Yan, S, Tyagi, RD and Surampalli, RY** 2015 Thermal pretreatment of sewage sludge to enhance anaerobic digestion: A review. *Crit Rev Env Sci Technol* **45**: 669–702. DOI: <https://doi.org/10.1080/10643389.2013.876527>
- Ploug, H** 2008 Cyanobacterial surface blooms formed by *Aphanizomenon* sp. and *Nodularia spumigena* in the Baltic Sea: small-scale fluxes, pH, and oxygen micro-environments. *Limnol Oceanogr* **53**: 914–921. DOI: <https://doi.org/10.4319/lo.2008.53.3.0914>
- Pogorzelski, SJ** 2001 Structural and thermodynamic characteristics of natural marine films derived from force-area studies. *Colloids and Surfaces A* **189**: 163–176. DOI: [https://doi.org/10.1016/S0927-7757\(01\)00584-2](https://doi.org/10.1016/S0927-7757(01)00584-2)
- Pogorzelski, SJ and Kogut, AD** 2001 Kinetics of marine surfactant adsorption at an air/water interface. Baltic Sea studies. *Oceanologia* **43**: 389–404.
- Pogorzelski, SJ and Kogut, AD** 2003 Structural and thermodynamic signatures of marine microlayer surfactant films. *J Sea Res* **49**: 347–356. DOI: <https://doi.org/10.1007/s00227-016-3042-4>
- Pogorzelski, SJ, Kogut, AD and Mazurek, AZ** 2005 Surface rheology parameters of source-specific surfactant films as indicators of organic matter dynamics. *Hydrobiologia* **554**: 67–81. DOI: <https://doi.org/10.1007/s10750-005-1007-6>
- Portela, R, Almeida, PL, Patrício, P, Cidade, T, Sobral, RG and Leal, CR** 2013 Real-time rheology of actively growing bacteria. *Phys Rev E* **87**: 030701(R). DOI: <https://doi.org/10.1103/PhysRevE.87.030701>
- Pravdić, V and Dragčević, D** 1985 Natural and man-made surface films at the air-sea interface: criteria based on measurements of physical phenomena. Lucerne, Switzerland: VII^e Journées d'Études sur les Pollutions CIESM, 53–62.
- Quesada, I, Chin, W-C and Verdugo, P** 2006 Mechanisms of signal transduction in photo-stimulated secretion in *Phaeocystis globosa*. *FEBS Lett* **580**: 2201–2206. DOI: <https://doi.org/10.1016/j.febslet.2006.02.081>
- Riebesell, U** 1992 The formation of large marine snow and its sustained residence in surface waters. *Limnol Oceanogr* **37**: 63–76. DOI: <https://doi.org/10.4319/lo.1992.37.1.0063>
- Rothstein, JP** 2010 Slip on superhydrophobic surfaces. *Ann Rev Fluid Mech* **42**: 89–209. DOI: <https://doi.org/10.1146/annurev-fluid-121108-145558>
- Sabbaghzadeh, B, Upstill-Goddard, RC, Beale, R, Pereira, R and Nightingale, PD** 2017 The Atlantic Ocean surface microlayer from 50°N to 50°S is ubiquitously enriched in surfactants at wind speeds up to 13 m s⁻¹. *Geophys Res Lett* **44**: 2852–2858. DOI: <https://doi.org/10.1002/2017GL072988>
- Schilling, K and Zessner, M** 2011 Foam in the aquatic environment. *Water Res* **45**: 4355–4366. DOI: <https://doi.org/10.1016/j.watres.2011.06.004>
- Schlichting, HE** 1974 Periodicity and seasonality of airborne algae and protozoa. In: Lieth, H (ed.), *Phenology and Seasonality Modeling*, 407–413. Berlin, Springer. DOI: https://doi.org/10.1007/978-3-642-51863-8_35
- Seuront, L, Lacheze, C, Doubell, MJ, Seymour, JR, Van Dongen-Vogels, V, et al.** 2007 The influence of *Phaeocystis globosa* on microscale spatial patterns of chlorophyll *a* and bulk-phase seawater viscosity. *Biogeochem* **83**: 173–188. DOI: <https://doi.org/10.1007/s10533-007-9097-z>
- Seuront, L, Leterme, SC, Seymour, JR, Mitchell, JG, Ashcroft, D, et al.** 2010 Role of microbial and phytoplanktonic communities in the control of seawater viscosity off East Antarctica (30–80°E). *Deep Sea Res II* **57**: 877–886. DOI: <https://doi.org/10.1016/j.dsr2.2008.09.018>
- Seuront, L, Vincent, D and Mitchell, JGB** 2006 Biologically induced modification of seawater viscosity in the Eastern English Channel during a *Phaeocystis globosa* bloom. *J Mar Syst* **61**: 118–133. DOI: <https://doi.org/10.1016/j.jmarsys.2005.04.010>
- Sieburth, JM** 1983 Microbiological and organic-chemical processes in the surface and mixed layers. In: Liss, PS and Slinn, WGN (eds.), *Air-Sea Exchange of Gases and Particles* **108**: 121–172. NATO ASI Series (Series C: Mathematical and Physical Sciences). Dordrecht: Springer. DOI: https://doi.org/10.1007/978-94-009-7169-1_3
- Sinterface Technologies** 2017 Interfacial Shear Rheometer ISR-1. http://sinterface.de/products/measurement/interfacial_rheology/interfacial_shear_rheology/isr1/index.html (Consulted 12 January 2018).
- Smetacek, V and Zingone, A** 2013 Green and golden seaweed tides on the rise. *Nature* **504**: 84–88. DOI: <https://doi.org/10.1038/nature12860>
- Smith, WO, Dennett, MR, Mathot, S and Caron, DA** 2003 The temporal dynamics of the flagellated and colonial stages of *Phaeocystis antarctica* in the Ross Sea. *Deep-Sea Res II* **50**: 605–617. DOI: [https://doi.org/10.1016/S0967-0645\(02\)00586-6](https://doi.org/10.1016/S0967-0645(02)00586-6)
- Soloviev, A and Lukas, R** 2014 Sea surface microlayer. In: Soloviev, A and Lukas, R (eds.), *The Near-Surface Layer of the Ocean*, 71–152. Dordrecht: Springer. DOI: https://doi.org/10.1007/978-94-007-7621-0_2
- Sonnenburg, J, Gao, J and Weiner, JH** 1990 Molecular dynamics simulations of gas diffusion through polymer networks. *Macromolecules* **23**: 4653–4657. DOI: <https://doi.org/10.1007/s10533-007-9097-z>
- Thorpe, S, Bowyer, P and Woolf, D** 1992 Some factors affecting the size distributions of oceanic bubbles.

How to cite this article: Jenkinson, IR, Seuront, L, Ding, H and Elias, F 2018 Biological modification of mechanical properties of the sea surface microlayer, influencing waves, ripples, foam and air-sea fluxes. *Elem Sci Anth*, 6: 26. DOI: <https://doi.org/10.1525/elementa.283>

Domain Editor-in-Chief: Jody W. Deming, Department of Biological Oceanography, University of Washington, US

Associate Editor: Laurenz Thomsen, Department of Earth and Space Sciences, Jacobs University Bremen, DE

Knowledge Domain: Ocean Science

Part of an *Elementa* Special Feature: The Sea Surface Microlayer – Linking the Ocean and Atmosphere

Submitted: 19 April 2017 **Accepted:** 20 January 2018 **Published:** 16 March 2018

Copyright: © 2018 The Author(s). This is an open-access article distributed under the terms of the Creative Commons Attribution 4.0 International License (CC-BY 4.0), which permits unrestricted use, distribution, and reproduction in any medium, provided the original author and source are credited. See <http://creativecommons.org/licenses/by/4.0/>.